Regional variations in provenance and abundance of ice-rafted clasts in Arctic Ocean sediments: implications for the configuration of late Quaternary oceanic and atmospheric circulation in the Arctic

R. L. Phillips
U.S. Geological Survey, lphillips@octopus.wr.usgs.gov

A. Grantz
Stanford University

ELSEVIER

Marine Geology 172 (2001) 91–115

MARINE GEOLOGY
INTERNATIONAL JOURNAL OF MARINE GEOLOGY, GEOCHEMISTRY AND GEOPHYSICS

www.elsevier.nl/locate/margeo

Regional variations in provenance and abundance of ice-rafted clasts in Arctic Ocean sediments: implications for the configuration of late Quaternary oceanic and atmospheric circulation in the Arctic

R.L. Phillips[a,*], A. Grantz[b]

[a]US Geological Survey, 345 Middlefield Road, MS 999, Menlo Park, CA 94025, USA
[b]Department of Geological and Environmental Sciences, Stanford University, Stanford, CA 94305-2115, USA

Received 2 June 1999; accepted 25 July 2000

Abstract

The composition and distribution of ice-rafted glacial erratics in late Quaternary sediments define the major current systems of the Arctic Ocean and identify two distinct continental sources for the erratics. In the southern Amerasia basin up to 70% of the erratics are dolostones and limestones (the Amerasia suite) that originated in the carbonate-rich Paleozoic terranes of the Canadian Arctic Islands. These clasts reached the Arctic Ocean in glaciers and were ice-rafted to the core sites in the clockwise Beaufort Gyre. The concentration of erratics decreases northward by 98% along the trend of the gyre from southeastern Canada basin to Makarov basin. The concentration of erratics then triples across the Makarov basin flank of Lomonosov Ridge and siltstone, sandstone and siliceous clasts become dominant in cores from the ridge and the Eurasia basin (the Eurasia suite). The bedrock source for the siltstone and sandstone clasts is uncertain, but bedrock distribution and the distribution of glaciation in northern Eurasia suggest the Taymyr Peninsula-Kara Sea regions. The pattern of clast distribution in the Arctic Ocean sediments and the sharp northward decrease in concentration of clasts of Canadian Arctic Island provenance in the Amerasia basin support the conclusion that the modern circulation pattern of the Arctic Ocean, with the Beaufort Gyre dominant in the Amerasia basin and the Transpolar drift dominant in the Eurasia basin, has controlled both sea-ice and glacial iceberg drift in the Arctic Ocean during interglacial intervals since at least the late Pleistocene. The abruptness of the change in both clast composition and concentration on the Makarov basin flank of Lomonosov Ridge also suggests that the boundary between the Beaufort Gyre and the Transpolar Drift has been relatively stable during interglacials since that time. Because the Beaufort Gyre is wind-driven our data, in conjunction with the westerly directed orientation of sand dunes that formed during the last glacial maximum on the North Slope of Alaska, suggests that atmospheric circulation in the western Arctic during late Quaternary was similar to that of the present. © 2001 Elsevier Science B.V. All rights reserved.

Keywords: Arctic Ocean; Ocean currents; Glacial transport; Clasts; Sedimentation

1. Introduction

The composition and distribution of ice-rafted erratics (clasts >2 mm) in box and piston cores provide information on the major Holocene and

* Corresponding author. Tel.: +1-650-329-5378; fax: +1-650-329-5299.
E-mail address: lphillips@octopus.wr.usgs.gov (R.L. Phillips).

0025-3227/01/$ - see front matter © 2001 Elsevier Science B.V. All rights reserved.
PII: S0025-3227(00)00101-8

upper Pleistocene current transport systems of the Arctic Ocean. Previous investigations of ice rafting, sediment composition, and provenance of ice-rafted sediment in the Arctic Ocean based on the gravel-sized fraction are limited. Such deposits in the central Arctic Ocean were investigated by Schwarzacher and Hunkins (1961); Clark et al. (1980); Clark and Hanson (1983) and shelf gravels in the Beaufort Sea were investigated by Rodeick (1979), and Mowatt and Naidu (1989). Vassmyr and Vorren (1990) examined the coarse fraction of glacial ice-rafted clasts from cores obtained in the southern Barents Sea, and they present a detailed lithologic description of clast composition and relate the clasts to adjacent glaciated terranes.

More recently Darby and Bischof (1996); Bischof et al. (1996) and Bischof and Darby (1997) identified sediment composition and potential sources of the fine-grain ice-rafted component ($>250\ \mu m$ or $250-300\ \mu m$ size fractions) in cores from the Amerasia basin. Most studies of ice-rafting in the Eurasia basin have also concentrated on the fine-grain fraction (Pfirman et al., 1989, 1990; Bischof, 1990; Nürnberg et al., 1994; Nørgaard-Pedersen, 1997; Landa et al., 1998).

The present surface-current regime of the Arctic Ocean (Fig. 1), which controls the movement of sea-ice and glacial icebergs, is dominated by the clockwise Beaufort Gyre in the Amerasia basin and by the east flowing Transpolar Drift in the Eurasia basin (Colony and Thorndike, 1984; Rigor, 1992). Bischof and Darby (1997) suggest that the Beaufort Gyre is only a Holocene phenomenon, and that during Pleistocene glacial intervals the surface circulation in the eastern Amerasia basin was in the opposite direction (Bischof et al., 1996). Observations by Nørgaard-Pedersen (1997) on the other hand, indicate that the observed ice-rafted debris (IRD) pattern from cores obtained in the central Arctic Ocean is consistent with the present circulation of the Beaufort Gyre and Transpolar Drift. The sharp boundary that separates carbonate-rich and siliciclastic-rich sediment on Lomonosov Ridge is considered by Nørgaard-Pedersen (1997) to be the result of transportation in two separate major current systems.

We present lithologic evidence that the major current systems of the Arctic Ocean, the Beaufort Gyre and the Transpolar Drift, have been in place during interglacial intervals of the Late Pleistocene and Holocene. In our study we examine the coarse sediment fraction, which was transported mainly by glacial icebergs, although we acknowledge that gravel-size clasts can also be transported by sea-ice, as reported by Reimnitz et al. (1992); Nürnberg et al. (1994).

We use the term ‘interglacial’ in a broad sense to represent periods of warming when the sea-ice sheet that formed during glacial periods in the Arctic Ocean melted and broke up allowing glacial icebergs as well as sea-ice to circulate freely. Evidence for a thickened Arctic Ocean sea-ice cover in the central Arctic Ocean during glacial periods includes restricted productivity and low sedimentation rates in the recurring stratigraphic intervals of Arctic cores that correspond with glaciation (Clark, 1971; Poore et al., 1993, 1999; Darby et al., 1997; Gard, 1988; Eisenhauer et al., 1994; Ishman et al., 1996; Nørgaard-Pedersen et al., 1998; Phillips et al., 1992; Phillips and Grantz, 1997). Glacial icebergs were able to circulate freely beyond the margins of the Arctic Ocean only when the sea-ice sheet that formed in the central Arctic during glacial stages melted and broke up during interglacial stages.

2. Methods

The cores were obtained from the USCGC *Polar Sea* in 1994 during a transpolar transect from the Chukchi Sea to the Eurasia basin (Fig. 1); in 1988, 1989, 1992, and 1993 on cruises of the USCGC *Polar Star* to the Beaufort Sea, Canada basin, and Northwind Ridge; and from the NOAA ships *Surveyor* in 1984, and *Discoverer* in 1985 in the Chukchi Sea (Table 1).

Undisturbed sediment samples from Northwind Ridge, the central Arctic Ocean, and the Chukchi Sea were obtained with a 40 x 40 x 60 cm box corer (Table 1). Vertical slices were made of the 1994 box cores to obtained 19 l subsamples and PVC tubes 8.5 cm in diameter were used to obtain approximately 5 l subsamples from the box cores from the Beaufort and Chukchi Seas. Piston cores 94PC-15 and 92PC-38, 8.5 cm in diameter, were X-rayed and subsampled to determine the gravel-size compositions from the initiation of glacial-ice rafting at approximately 2.7 Ma in the western Arctic Ocean.

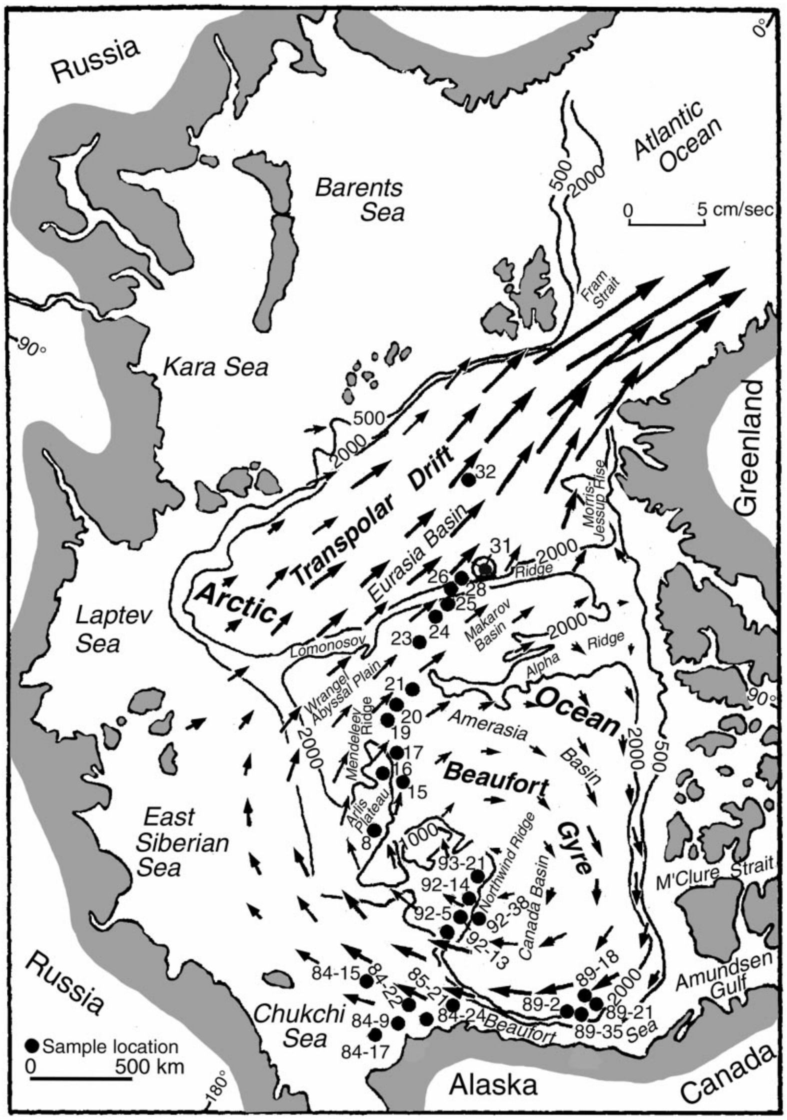

Fig. 1. Arctic Ocean showing location of box and piston cores and major current systems in the Arctic Ocean (from Rigor, 1992), the clockwise Beaufort Gyre and the east to west flowing Transpolar Drift. Core numbers lacking a year prefix collected in 1994. See Table 1 for core type, location and depth. Depth contours in meters.

Subsamples representing the entire stratigraphic section in each box core were wet sieved to retain the >2.0 mm size fraction. The gravel fraction of each subsample, consisting of 187 to 2035 clasts, was then counted and identified as to lithologic composition with a binocular microscope. Vertical sections of the box cores 2 cm thick were X-rayed to determine the distribution of the gravel-size clasts. Correlation of the central Arctic cores was achieved by integrating the X-rays, core logger data, published ^{14}C dates, and observed lithostratigraphy. Only clast compositional data, however, were obtained on the Chukchi Sea box cores and three of the Beaufort Sea box cores.

Table 1
Location, length, and depth of cores. PC in core number designates piston core, BC designates box core. All Arctic Ocean cores were collected by the authors during US Geological cruises on the US Coast Guard Cutters Polar Star in 1988, 1989, 1992, and 1993 and Polar Sea in 1994

Core number	Depth (m)	Length (cm)	Core location	Area	Clasts/l
Central Arctic Ocean, 1994					
94BC-8	1031	42	78° 07.68′ 176° 44.67′	Arlis Plateau	100
94PC-15	2700	772	80° 13.53′ 173° 19.19′	Mendeleev Ridge	
94BC-16	1500	42	80° 20.03′ 178° 40.05′	Mendeleev Ridge	82
94BC-17	2217	46	81° 15.91′ 178° 58.05′	Mendeleev Slope	38
94BC-19	2400	43	82° 26.80′ 175° 45.50′	Mendeleev Slope	32
94BC-20	3110	40	83° 10.20′ 174° 06.36′	Wrangel Abyssal Plain	23
94BC-21	3193	42	84° 05.72′ 174° 57.82′	Wrangel Abyssal Plain	15
94BC-23	3475	42	85° 54.40′ 166° 41.00′	Makarov basin	13
94BC-24	3890	48	87° 09.70′ 161° 02.20′	Makarov basin	10
94BC-25	2125	33	88° 03.30′ 147° 40.80′	Lomonosov Slope	31
94BC-26	1020	36	88° 48.60′ 142° 58.90′	Lomonosov Ridge	20
94BC-28a	1990	45	88° 52.40′ 140° 10.80′	Lomonosov Slope	42
94PC-28b	1980	480	88°52.39′ 140° 22.58′	Lomonosov Slope	
94PC-31	4180	837	89° 58.08′ 47° 35.00′	Pole Abyssal Plain	
94BC-32	3450	53	85° 43.04′ 37° 44.52′	Barents Abyssal Plain	26
Northwind Ridge, 1992/1993					
92BC-5	1239	40	73° 59.50′ 159° 53.00′	Northwind Ridge	286
92BC-13	1206	38	74° 59.30′ 157° 38.80′	Northwind Ridge	226
92BC-14	690	37	76° 16.05′ 156° 35.60′	Northwind Ridge	175
93BC-21	1470	41	76° 51.80′ 154° 12.86′	Northwind Ridge	148
93PC-21	1470	683	76° 51.80′ 154° 12.86′	Northwind Ridge	
92PC-30	765	767	75° 18.70′ 158° 02.78′	Northwind Ridge	
92PC-38	1917	690	75° 51.98′ 155° 41.89′	Northwind Ridge	
92PC-40	700	548	76° 15.51′ 156°32.86′	Northwind Ridge	
Beaufort Sea, 1989					
89BC-2	2800	30	71° 07.70′ 143° 01.20′	Canada basin	
89BC-18	2909	30	71° 19.52′ 142° 01.10′	Canada basin	948
89BC-21	2591	21	71° 09.70′ 142° 04.52′	Beaufort Sea Slope	
89BC-35	2072	40	70° 59.91′ 142° 02.49′	Beaufort Sea Slope	
Chukchi Sea, 1984					
84BC-9	39	11	70° 65.83′ 162° 16.33′	Chukchi Sea	
84BC-15	44	28	70° 58.80′ 167° 44.20′	Chukchi Sea	
84BC-17	43	30	70° 41.00′ 166° 47.50′	Chukchi Sea	
84BC-22	42	13	71° 02.00′ 161° 36.33′	Chukchi Sea	
84BC-24	37	30	70° 46.60′ 160° 05.40′	Chukchi Sea	
Chukchi Sea slope, 1985					
85BC-21	80	22	71° 00.9′ 159° 16.00′	Chukchi Sea	

3. Stratigraphy

The stratigraphy of the cores is variable, depending on local sedimentation rates, physiographic position, and modification of the dominantly ice-rafted sediments by contour currents on the ridges and turbidite deposition in the basins. Box cores from the Amerasia basin contain as many as three brown beds with abundant foraminifers separated by olive gray beds that lack or contain greatly reduced numbers of foraminifers (Darby et al., 1997; Poore et al., 1999). The brown beds are intensely bioturbated dark yellowish brown to grayish brown mud while the olive gray beds lack, or contain only rare intervals of bioturbated yellowish gray mud.

The uppermost (first) foraminifera-rich brown bed in the box cores is 2–11 cm thick and represents Holocene sedimentation (Fig. 2). ^{14}C dates of planktic

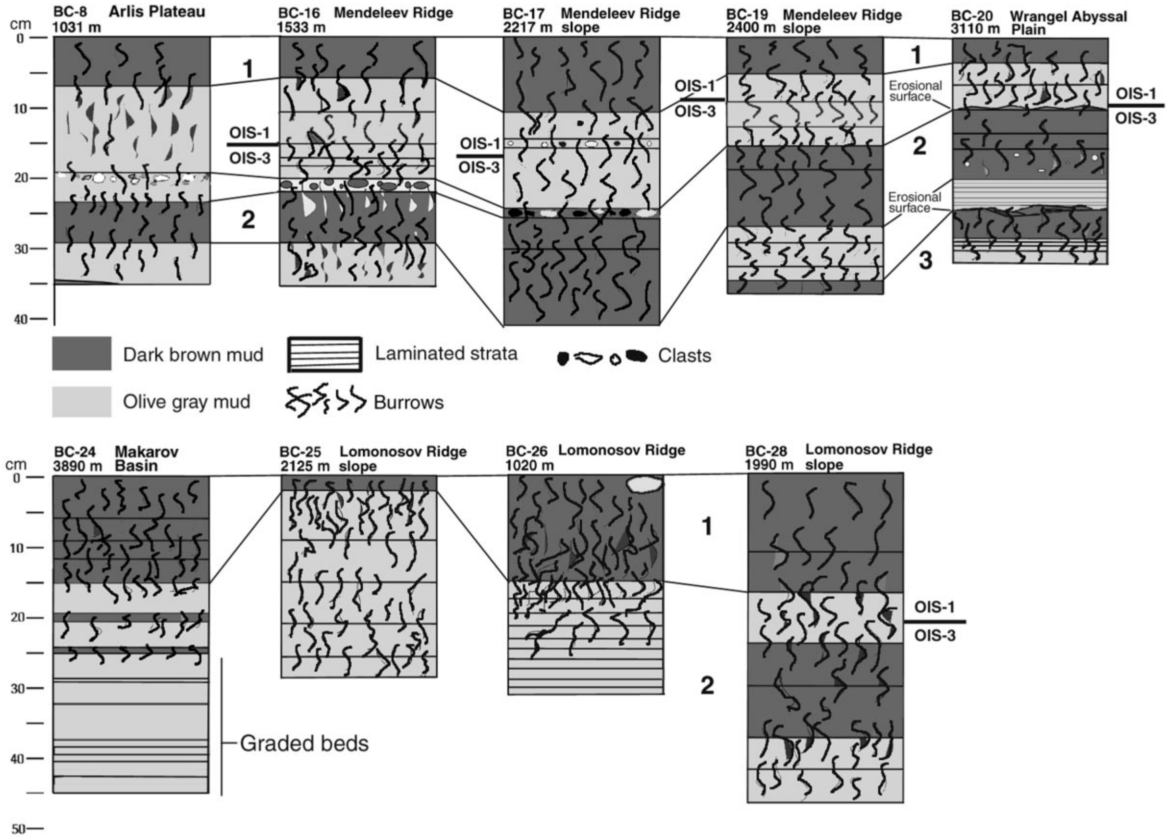

Fig. 2. Lithostratigraphy and correlation of strata in the 1994 box cores from the Amerasia Basin and Lomonosov Ridge. The correlative brown beds are labeled 1, 2, and 3. OIS-1 and OIS-3 (oxygen isotope stage) boundaries for cores 94BC-16, 94BC-17, and 94BC-19 from Poore et al. (1999); the OIS-1 and OIS-3 stage boundaries for cores 94BC-20 and 94BC-28 determined from ^{14}C dates in Darby et al. (1997). Intense bioturbation in the brown beds has created burrows in the olive gray mud that are filled with foraminifer-rich brown mud 7 to 10 cm below the base of the brown beds.

foraminifera by Poore et al. (1999) for three of the 1994 box cores indicate that the base of the first (upper) brown bed varies in age from 9610 in 94BC-16, to 11,250 in 94BC-17, and 11,680 years in 94BC-19; and from data in Darby et al. (1997) we identify the ^{14}C ages of the first brown bed as 9580 years in 94BC-20 and 11,560 years in 94BC-28. The second brown bed is 6–10 cm thick. ^{14}C dates range from 31,490 to 36,530 years at the top of the second brown bed to 41,870–44,160 years at its base in box cores 94BC-16, 94BC-17, and 94BC-19 (Poore et al., 1999). Data in Darby et al. (1997) indicate ^{14}C ages of 27,000 and 39,060 years near the top of the second brown bed and 42,560 and 44,960 years near the base of this bed. The upper part of the third brown bed is found in box cores 94BC-8 and 94BC-19. The third brown bed is 4 cm thick in box core 94BC-20 and contains an irregular upper surface with small-scale crossbeds indicating some erosion and reworking of the top of this bed (Fig. 2). The third brown bed is beyond the range of ^{14}C dating. Poore et al. (1999) indicate that the oxygen isotope stage 3 (OIS-3) to OIS-4 transition may occur above the third brown bed in core 19 suggesting that the brown bed represents OIS-5.

Differences in interpretation of the depositional environments of the 1994 cores appear to exist between Darby et al. (1997) and Poore et al. (1999). Based on foraminiferal peaks, ^{14}C dating, and oxygen and carbon isotopes Poore et al. (1999) recognize

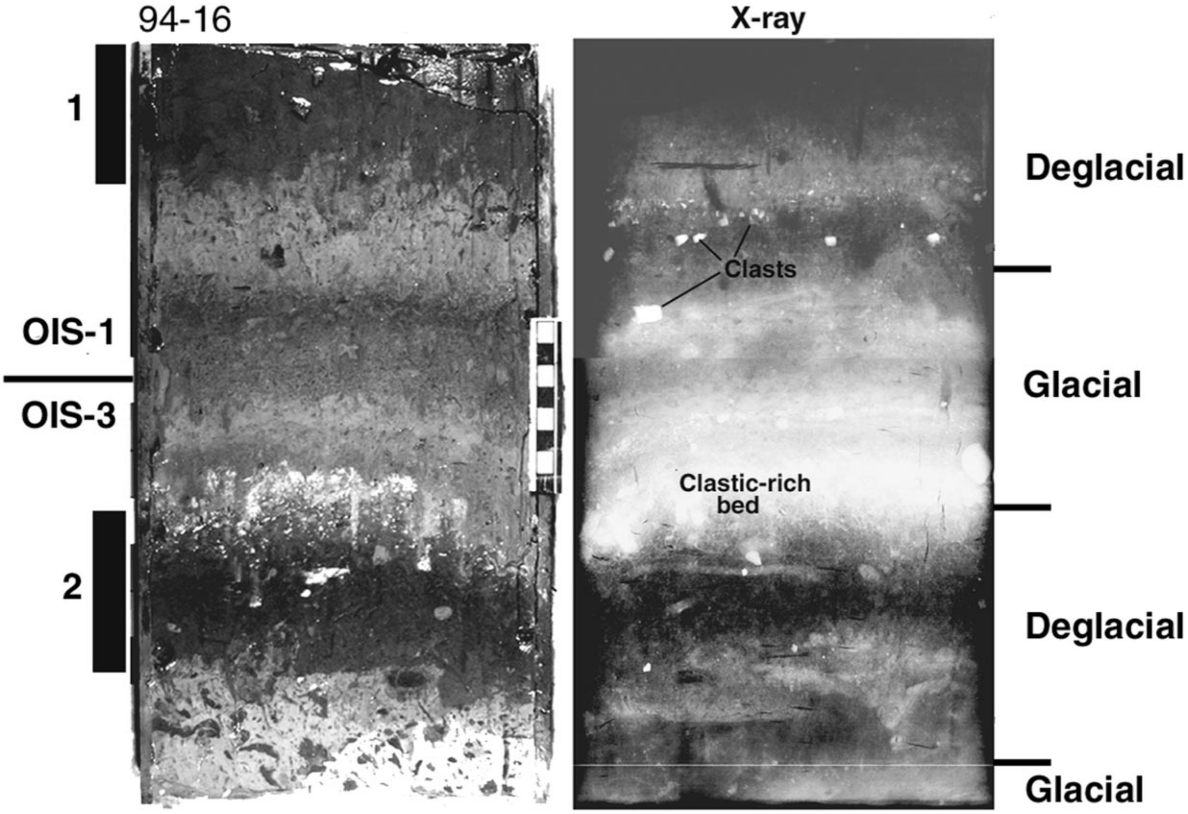

Fig. 3. Photograph (left) and X-ray of box core 94BC-16 from Mendeleev Ridge at 1533 m water depth. OIS-1 and OIS-3 boundaries from Poore et al. (1999), the glacial and deglacial units from Darby et al. (1997). Black bars on left indicate the brown beds. Clasts are white in the X-ray. Note clastic-rich bed located at top of second brown bed. Scale bar in centimeters.

OIS-1 and OIS-3 in box cores 94BC-16, 94BC-17, and 94BC-19. OIS-2, representing the last glacial period, is either very thin, bioturbated by fauna originating in the overlying interglacial unit and mixed, or may have been eroded as suggested by Poore et al. (1999) from the presence of a coarse-grained lag deposit in the upper 5 cm of OIS-3 (Fig. 3). Darby et al. (1997) based on ^{14}C dating, foraminifera distribution, and clastic content identifies as many as three glacial deposits bounded by 'deglacial' beds within the 1994 box cores (Fig. 3).

The age of the brown beds in our box cores from the Eurasia basin is apparently similar to that of the Amerasia basin cores. Nørgaard-Pedersen et al. (1998) report that cores on Lomonosov Ridge contain foraminifera peaks that belong to OIS-1 and OIS-3, with strata extending to OIS-4/5 at depths of 36–39 cm. Among our cores from Lomonosov Ridge, box cores 94BC-25 and 94BC-26 contain one brown bed and core 94BC-28 contains two brown beds with foraminifers. The upper brown bed in these cores is Holocene, whereas, the second brown bed contains a ^{14}C date of 44,960 years Darby et al. (1997). Box core 94BC-32 may extend to OIS-2/3 within the turbidite deposits of Eurasia basin at the base of the core. The gravel clasts in our box cores, therefore, represent composite sample of ice-rafted clasts from the Holocene and upper Pleistocene as far back as OIS-5 and include sediment deposited in both interglacial and glacial environments.

Gravel distribution in the cores is variable (Fig. 3). X-rays indicate that clasts are especially abundant in the basal beds of each depositional cycle, but they are scattered throughout some of the brown beds, and may occur at the top of a brown bed, as seen in the top of OIS-3 in Fig. 3. The clasts decrease in abundance toward the top of most of the brown beds.

Coarse-grained IRD is transported and released in the Arctic Ocean by glacial icebergs during glacial periods (Bischof et al., 1996; Bischof and Darby, 1997), or during continental glaciations and deglaciations (Darby et al., 1997). Studies of the 1994 box cores by Darby et al. (1997) state that during glacial periods the IRD content is low and variable and is associated with periods of low foraminifera productivity. We agree with Bischof et al. (1996), Bischof and Darby (1997), and Darby et al. (1997) that the coarse-grained IRD is mainly transported by glacial ice, but, we differ as to when the glacial icebergs were free to move within the western Arctic Ocean and deposit the coarse-grained IRD.

In contrast to work by Bischof and Darby (1997) our studies indicate that most of the glacial erratics in central Arctic Ocean sediments were deposited in the early part of interglacial periods, when icebergs could circulate freely across the central Arctic Ocean but the waning Laurentide ice sheet was still sufficiently robust to calve icebergs into the Amerasia basin (Phillips and Grantz, 1997). Our model for the environmental conditions present during alternating glacial and interglacial cycles in the Amerasia basin are presented in Fig. 4. During synglacial times, the sea-ice thickened and excluded erratic-bearing icebergs from the central Arctic basin and erratics are generally absent from the gray synglacial late Quaternary deposits of the region. During glacial periods continental glaciers built up over northern Canada and extended to and entered the Arctic Ocean, but, a thickening sheet of sea-ice, at least over the western Arctic Ocean, restricted the glacial icebergs to its margins. The thick sea-ice cover also restricted sunlight, oxygen and therefore primary photosynthetic biological productivity in the Arctic Ocean. This resulted in the deposition of usually laminated gray silt and clay essentially lacking both fauna and coarse-grained IRD during each successive glaciation in the Arctic basin (Fig. 4).

During the initial warming stage of interglacials in the Arctic Ocean the sea-ice sheet thinned and broke up, allowing glacial icebergs to circulate, melt, and deposit sand, silt, and clay as well as coarse-grain IRD. This is reflected by the deposition of gravel-rich oxic beds containing rare to abundant planktic and benthic fauna directly upon each foraminifera- and IRD-poor laminated gray strata deposited during the proceeding glacial interval. Coarse IRD deposition decreases upsection in each well oxygenated, foraminifer- and IRD-rich brown bed and are supplanted by increasing amounts of sea-ice-rafted sand-size sediment. The brown beds represent deposition during periods of a well ventilated water column during interglacials (Phillips and Grantz,, 1997; Poore et al., 1993, 1999; Jakobsson et al., 2000). The abrupt termination of the brown beds and foraminifers records a significant, as well as an abrupt increase in sea-ice thickness at the start of the next glacial stage. An influx of coarse-grained IRD may be found in this interval at the top of the brown beds or within the laminated olive gray beds directly overlying the brown beds in some depositional cycles. These IRD events apparently record surges of glacial icebergs into the central Arctic Ocean before some of the sea-ice sheets were fully developed. The association of planktic fauna with some of these events suggests that they record brief warming events within the early phases of some glacial stages (Fig. 4).

Bischof et al. (1996), and Bischof and Darby (1997) suggest that much of the coarse-grain IRD in piston cores from the Amerasia Basin were deposited during glacial periods (six in the last million years). In contrast, Darby et al. (1997) indicate that much of the coarse IRD in the 1994 box cores was deposited during deglacial periods with variable amounts of IRD deposited during glacial periods. The 'deglacial' events of Darby et al. (1997) apparently correlate with the coarse IRD influx we see at the base of interglacial depositional cycles, but does not include the coarse-grained pulses we see within or near the top of the brown beds deposited during interglacial periods (Fig. 4).

Some workers (e.g. Darby et al., 1997; Clark, 1990) have used the term 'deglacial' to describe the beds with IRD in Arctic Ocean Quaternary deposits. We suggest the term is an inappropriate descriptor for these beds for two reasons. First because the retreat and collapse of continental glaciers during deglaciation is not a process that would produce an influx of glacial icebergs into the Arctic Ocean. Second, the lithostratigraphic record in the Amerasia basin (Phillips and Grantz, 1997) indicate that the presence of IRD in Arctic Ocean Quaternary deposits was controlled by processes operating on the surface the Arctic Ocean, namely the waxing and waning of a

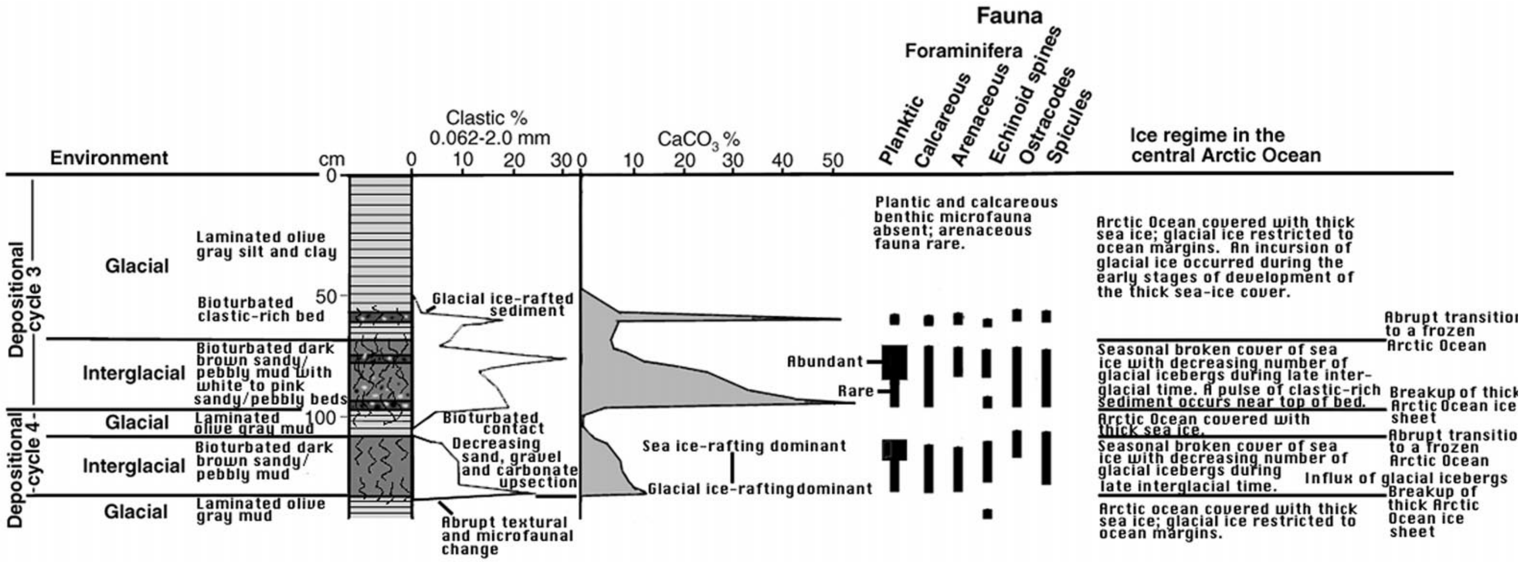

Fig. 4. Two lithostratigraphic cycles in piston core 92PC-30 from 765 m depth on Northwind Ridge, illustrating the distinct stratigraphic, textural, and faunal changes that impart cyclicity to the cores. An interpretation of the sea-ice conditions that produced the cyclicity from Phillips and Grantz (1997) is presented on the right. See Fig. 12 for core location.

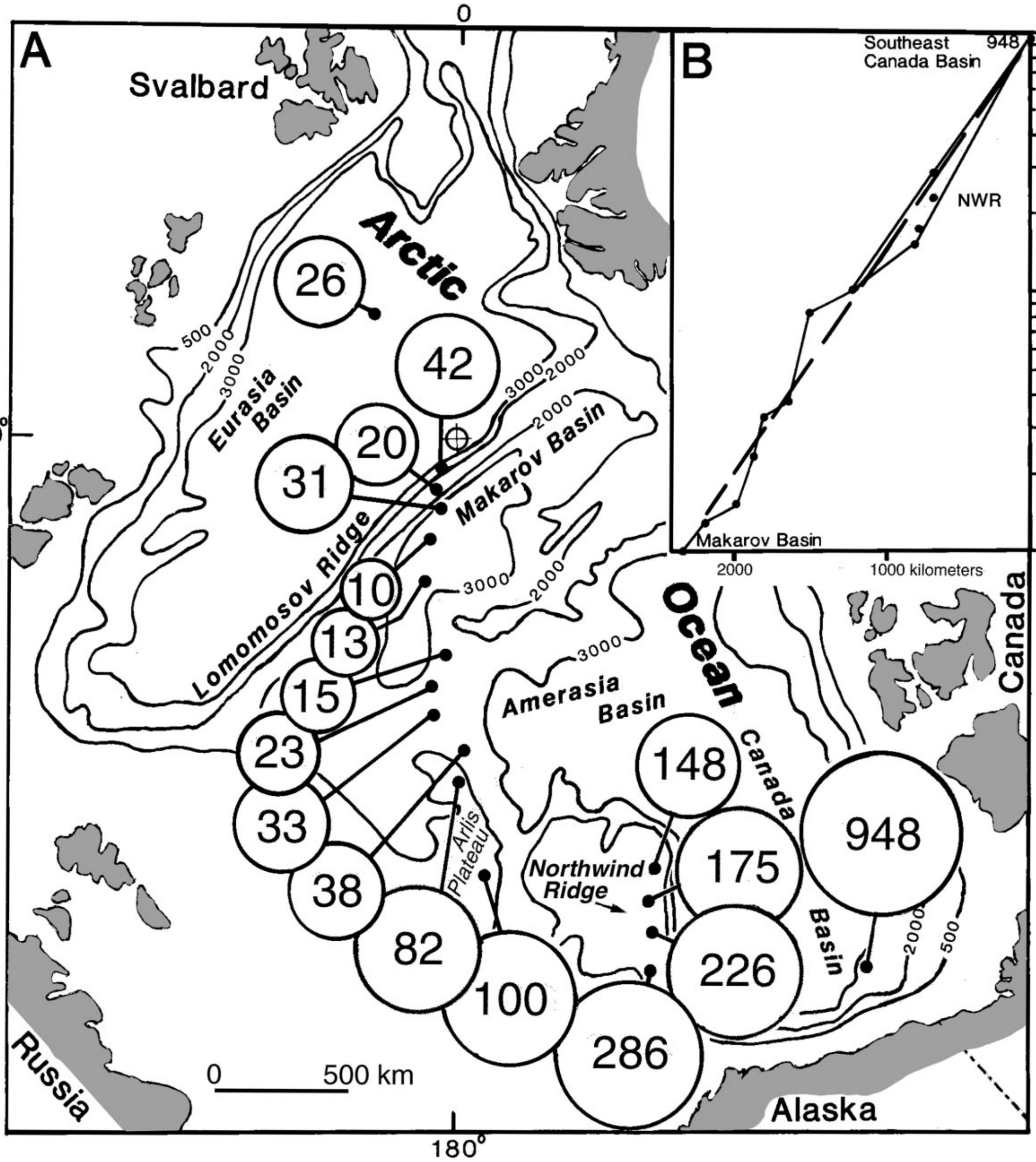

Fig. 5. A. Number of clasts >2.0 mm l^{-1} of sediment in box cores from the Arctic Ocean. B. Semilog plot of clast/liter vs sample distance from southeast Canada Basin near Canadian Arctic Islands to Makarov basin in central Arctic Ocean, showing a logarithmic decrease in clast abundance that resembles a glacial ice decay-gravel sedimentation function (see text). The logarithmic decrease in clast abundance with distance indicates that the source of the sediment-laden icebergs in the Beaufort Gyre was northwestern Canada. Depth contours in meters.

thick cover of floating sea-ice during glacial intervals, rather than processes acting solely within the continental ice sheets. IRD-bearing icebergs reached the central Amerasia basin in the early stages of each glacial episode, when the floating cover of sea-ice was still relatively thin. They also reached the central part of the basin during the late stages of each glacial cycle and the early stages of the

succeeding interglacial cycle, when the thick sea-ice cover was thinning but continental glaciers were still sufficiently vigorous to calf erratic-laden icebergs into the Arctic Ocean. Coarse-grained IRD is markedly less abundant, or absent, from the middle and upper part of interglacial intervals, when floating sea-ice sheet were absent and glacial icebergs were reduced in number, or even absent, over the Amerasia basin.

4. Clast concentration

Clast concentrations in our cores decrease by 89% from the southeast Canada basin to Arlis Plateau in the southern Amerasia basin, and by 98% from the southeast Canada basin to the Makarov basin near Lomonosov Ridge, which shows that most of the glacial IRD is deposited along the southern margin of the Amerasia basin (Table 1, Fig. 5). The highest concentrations of glacial ice-rafted clasts are found on the southeastern Canada basin and the Beaufort Sea slope adjacent to the Laurentide ice sheet, the region of Pleistocene continental glaciation in Arctic Canada (Dyke and Prest, 1989a,b). Thus, core 89BC-18, from the eastern Beaufort Sea, contains 948 clasts l^{-1} of sediment, the highest concentration encountered in our study. The decreasing concentrations of erratics in our cores with increasing distance from southeastern Canada basin to Mararov basin indicates the clasts originated in northwestern Canadian Arctic (Fig. 5).

It is of great significance that clast concentrations increase over the Amerasia flank of the Lomonosov Ridge near the North Pole, and that cores from both Lomonosov Ridge and the Eurasia basin contain relatively high clast concentrations. However, no distinct trends in clast concentrations can be discerned within these areas due to the limited number of cores.

5. Clast composition

Seven clast types were identified in our cores: (1) sandstone and siltstone; (2) quartz and chert; (3) limestone and dolostone; (4) metamorphic; (5) igneous; (6) coal; and (7) unknown (Figs. 6 and 7, Table 2). It was found that the clast suites from the Amerasia and Eurasia basins are lithologically distinct.

5.1. Amerasia clast suite

Detrital carbonate, which comprises as much as 70% of the clasts from the Amerasia basin but decreases northward to 34% in the Makarov basin, characterizes the Amerasia clast suite of the western Arctic Ocean (Figs. 6 and 7). The most abundant carbonate clast type is tan and light to dark brown microcrystalline dolostone that may contain glauconite, oolites, and in some clasts micro or macrofossils. The less abundant limestone clasts are usually white to cream-color and have a crystalline fabric.

Dolostone clasts are abundant within the gravel fraction in the Northwind Ridge and eastern Beaufort Sea cores (Phillips and Grantz, 1997), as well as in the surface sediments of the eastern Beaufort shelf (Rodeick, 1979). Dolostone and limestone clasts on Northwind Ridge comprises 31–56% of the gravel fraction in four late Pleistocene box cores from the ridge crest (Fig. 6), and range from 30 to 64% in interglacial units deposited during the last 1 Ma on Northwind Ridge (Phillips and Grantz, 1997). Carbonate clasts also comprise 36–70% of the erratic clasts in four cores from the late Quaternary section in the continental slope of the Beaufort Sea and adjacent Canada basin near 142° west longitude, and in a surface sample from the Chukchi Sea continental slope near 157° west longitude (Fig. 7). Rodeick (1979) found that dolostone and limestone comprise as much as 85% of the gravel and dolostone as much as 82% of the carbonate fraction in the 8–16 mm size clast fraction from surficial sediments on the outer Beaufort Sea shelf.

Sandstone and siltstone clasts increase from an average of 26% in four samples from the southeastern Canada basin to 46% in the northern most sample in the Makarov basin, where the concentration of the clastic rocks exceeds the carbonate component (Figs. 6 and 7). In the Canada basin cores sandstone and siltstone clasts are dominated by light to dark gray siltstone or fine-grained sandstone containing lignitic plant fragments and usually abundant mica, and by sandstone composed of well sorted, well rounded white or pink quartz grains. Sandstone clasts in the Makarov basin consist of fine-grained silty micaceous sandstone, as is common in the Amerasia basin sediments, but also coarse-grained sandstone rich in white quartz not found in cores from the Amerasia basin.

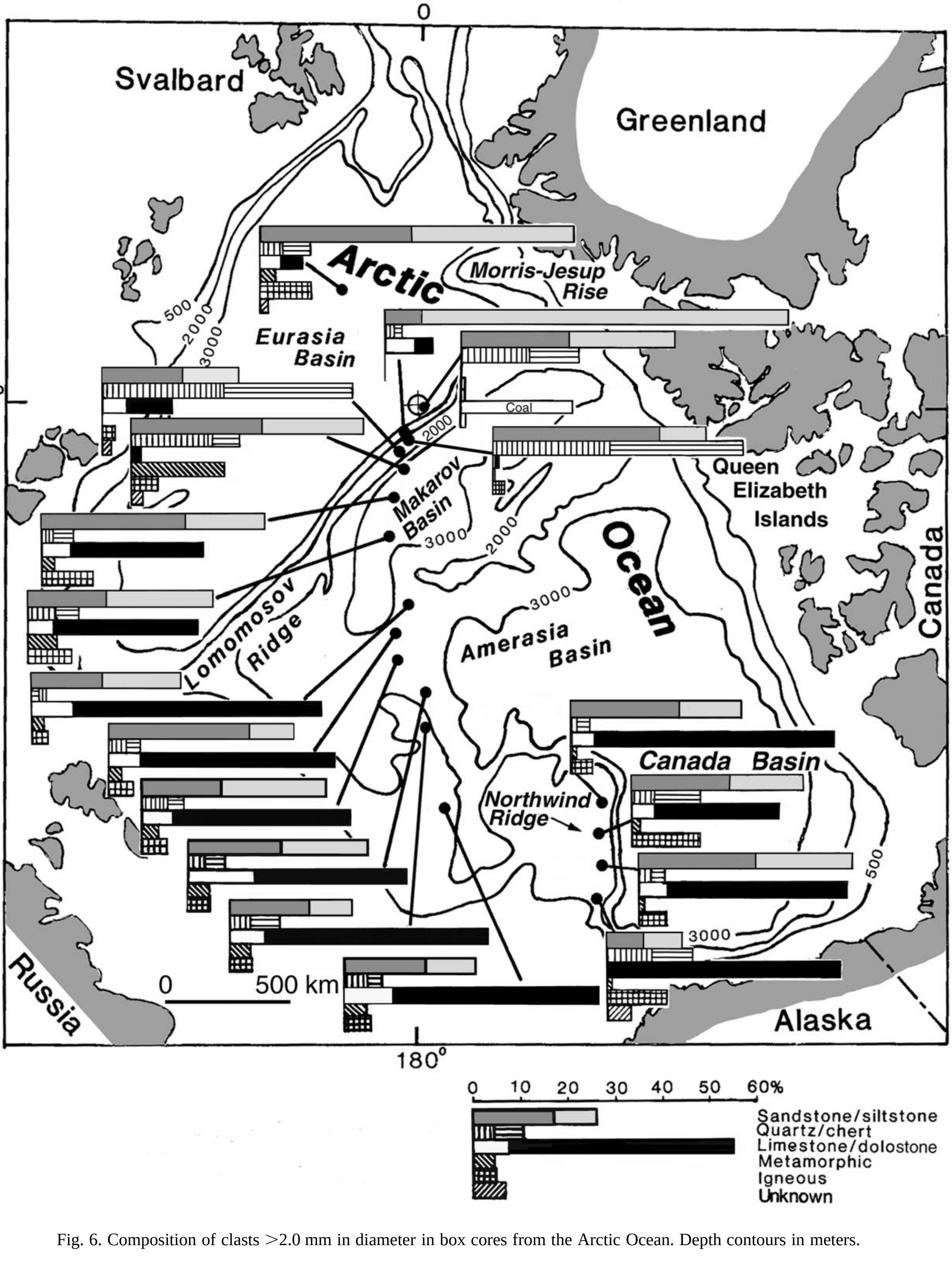

Fig. 6. Composition of clasts >2.0 mm in diameter in box cores from the Arctic Ocean. Depth contours in meters.

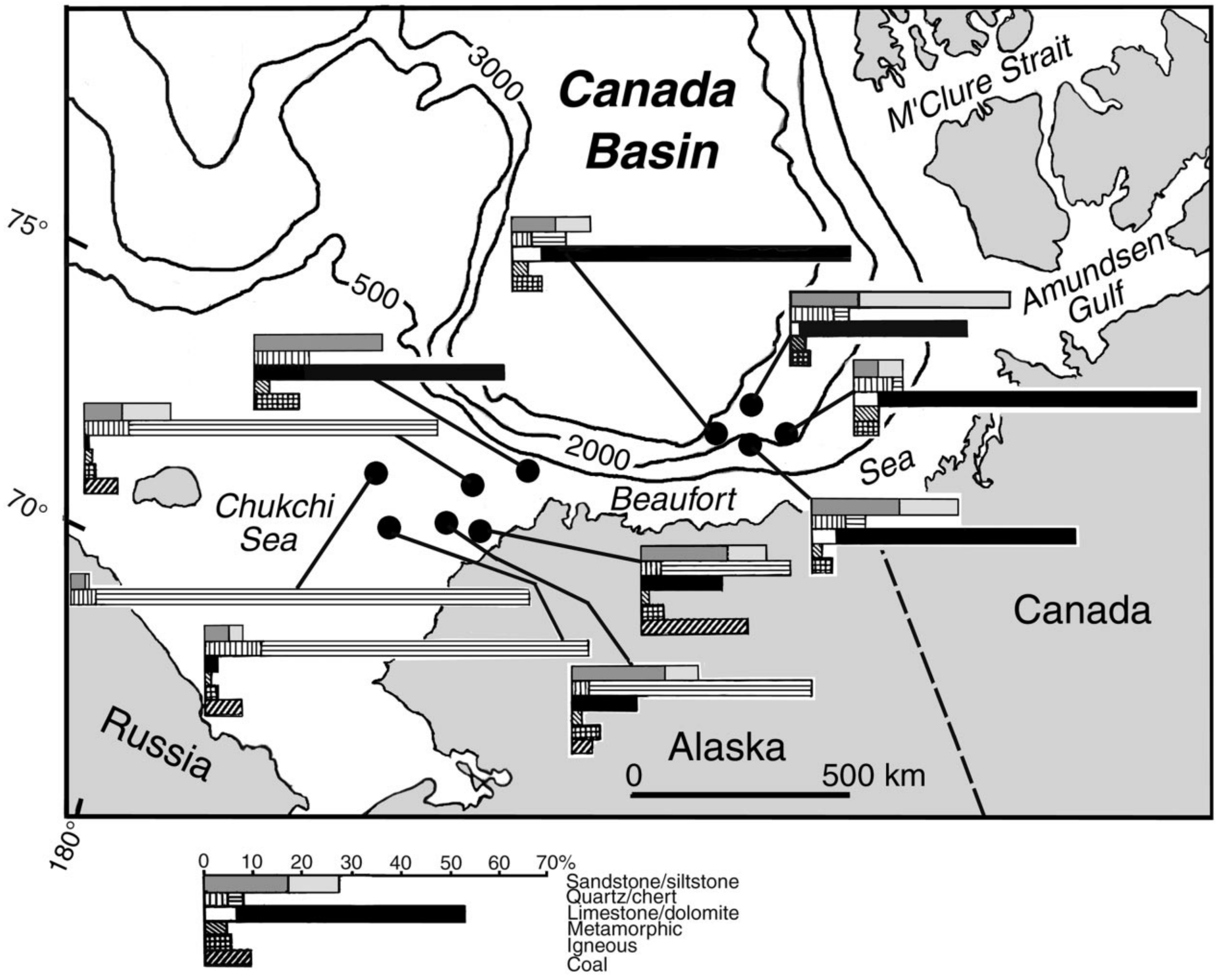

Fig. 7. Composition of clasts >2.0 mm in diameter from the Chukchi and Beaufort Seas. Depth contours in meters.

This indicates that the sandstone clasts from western Canada were mixed with clasts from another source in the vicinity of the Amerasia flank of the Lomonosov Ridge. The position of this zone of mixing at the junction of the Beaufort Gyre with the Transpolar Drift indicates that sandstone rich in white quartz was transported to the central Arctic in the Transpolar Drift and therefore originated in northern Russia.

Siliceous clasts (chert and quartz) comprise from 2.8 to 22.5% of the Amerasia clast suites, with the highest values found in the Makarov basin adjacent to Lomonosov Ridge. The siliceous clasts consist of well rounded to broken rounds of multicolored chert, which in some samples is fossiliferous, and clear to multicolored well rounded to angular quartz clasts with a coarse crystalline fabric. Quartz and chert clasts, dominated by well rounded black chert and white quartz, comprise as much as 95% of the clasts in the gravel fields of the Chukchi Sea shelf (Fig. 7). On the inner Beaufort Sea shelf chert clasts derived from the Brooks Range comprise up to 75% of the clasts (Rodeick, 1979).

Metamorphic and igneous clasts are minor but distinctive components of the gravel fraction. They include abundant angular green phyllite and rare quartz biotite gneiss, andesite, basalt, and pyroxenite. A distinctive pink to red granite similar to granitic

Table 2
Description of ice-rafted clasts >2.0 mm in late Quaternary sediments of the Arctic Ocean

Amerasia suite	
Sandstone	Rounded to subrounded clasts of light to dark gray, well sorted, sandstone with fine to medium-grain quartz and feldspar grains, biotite and black plant fragments (lignite); rare white or pink coarse-grained quartzite, or medium-grain quartz sandstone containing an orange matrix. Some clasts contain microfossils.
Siltstone	Angular clasts of light to dark gray siltstone with abundant mica and black plant fragments (lignite); rare dark reddish brown siltstone clasts.
Chert	Generally well rounded clasts to broken rounds of black, white, cream, light green, tan, yellow, or red chert that is commonly banded or may be brecciated. Some clasts contain microfossils.
Quartz	Usually well rounded clasts of white, cream, yellow, pink, or clear microcrystalline or polycrystalline quartz. Some clasts iron-stained.
Dolostone	Angular to subrounded clasts of white, light gray, tan, light brown (most abundant), to dark brown microcrystalline to coarse crystalline dolostone with glauconite, oolites, and micro- and mega-fossils. Large clasts exhibit laminations, thin beds and graded bedding.
Limestone	Angular to rounded clasts, usually white of microcrystalline limestone with some microfossils.
Metamorphic	Angular clasts of green, gray, to black phyllite or quartz-biotite gneiss.
Igneous	Predominately clasts of red to pink granite and coarse crystalline quartz diorite, with rare andesite, basalt, and pyroxenite.
Coal	Rare in most cores, but common in upper part of cores from Northwind Ridge, and the Chukchi and Beaufort Sea.
Eurasia suite	
Sandstone	Well rounded to rounded clasts of yellowish orange, yellowish brown, to orange sandstone; with white, cream, tan, light gray, and commonly light green poor to well sorted silty fine- to coarse-grained sandstone or quartzite. Some of the poorly sorted silty sandstones contain a tan to orange mud matrix. Surface voids common in medium- to coarse-grained quartz sandstones. An orange limonitic or black iron-manganese coating covers many of the clasts.
Siltstone	Subrounded clasts of yellow, tan, orange, brown, red, light gray, gray, to mottled red and yellow siltstone. The gray clasts contain biotite and fine black plant fragments (lignite).
Chert	Well rounded to subrounded clasts of gray, white, green and black chert.
Quartz	Well rounded clasts of white, yellow, to clear monocrystalline and polycrystalline quartz.
Dolomite	Subrounded to angular clasts of light gray, gray, tan, to light brown microcrystalline dolostone, some clasts oolitic.
Limestone	Subrounded clasts of white to yellow microcrystalline limestone.
Metamorphic	Subrounded to round clasts of light green, light gray, to gray phyllite, and subordinate blue garnet schist, mica schist, biotite gneiss, and gray to green metasediment clasts.
Igneous	Rounded to subrounded clasts of quartz diorite, hornblende granite, pink granite (rare), andesite, and altered (weathered) quartz-rich volcanic (rhyolite?) containing large spheroids filled with yellow clay.
Coal	Clasts of angular to subrounded black coal.

clasts in the Flaxman Member of the Gubik Formation of the North Slope of Alaska (Rodeick, 1979) is found in all Amerasia basin samples.

5.2. Eurasia clast suite

Clasts of sandstone and siltstone plus quartz and chert, which together constitute 71–88% of the gravel fraction, characterize the Eurasia clast suite of the eastern Arctic Ocean on Lomonosov Ridge near the North Pole and in the Eurasia basin (Fig. 6). The most abundant clast types are yellowish orange, brown, and orange poor to well sorted silty fine- to coarse-grain sandstone or quartzite (Table 2). The poorly sorted silty sandstone clasts usually contain a tan to orange mud matrix. A granule to pebble conglomerate consisting of well rounded quartz and fossiliferous chert clasts containing an orange sand matrix is locally abundant. Bischof (1990); Bischof et al. (1996) also reported that sandstone, siltstone, quartz, and quartzite are the most common dropstone lithologies in the Eurasia basin, and that clastic sedimentary rocks are the dominant clast in sediments from Fram Strait.

Concentrations of carbonate clasts, which constitute 31–70% of the gravel fraction in the Amerasia basin, fall abruptly to concentrations of 2–14% on Lomonosov Ridge and the Eurasia basin. The significance of this reduction in concentration of carbonate clasts is reinforced by a parallel change in composition of the carbonate fraction. Dolostone, which is everywhere

several times more abundant than limestone in the Amerasia basin, is only equal or subordinate to limestone on Lomonosov Ridge and in the Eurasia basin. A sharp reduction in the carbonate content and an increase in the sandstone and siltstone clasts between cores from the Makarov basin and the adjacent Lomonosov Ridge are also reported by Nørgaard-Pedersen (1997). Vogt (1996) reports concentrations of ice-rafted carbonate clasts of 17% on Lomonosov Ridge and carbonate concentrations of <10% are reported for the eastern Eurasia basin by Stein (1996). Bischof (1990) also finds that carbonate clasts are rare or missing in the upper Pleistocene sediments of the Eurasia basin and states that the presence or absence of carbonate distinguishes between ice-rafted debris from the Amerasia and Eurasia basins. On the other hand, Spielhagen et al. (1997) reports 30–60% detrital carbonate from OIS-3 to −5 in cores from Lomonosov Ridge crest and that high carbonate concentrations extend back into the Gilbert Chron.

Metamorphic clasts comprise 0–2.5% of most of the cores from Lomonosov Ridge and the Eurasia basin, but in one core on the Makarov basin flank of Lomonosov Ridge they constitute 19% of the gravel fraction (Fig. 6). Light green phyllite forms 9% of the clasts in this core, and mica schist, biotite gneiss, and gray-to-green metasediment are also present. A distinctive blue schist containing red garnets which was not seen (recognized) in the Amerasia clast suite is found only in cores from Lomonosov Ridge. Igneous clasts, which comprise 0–10% of the ice-rafted sediment in Lomonosov Ridge and Eurasia basin cores, are rounded to subrounded and include quartz diorite and fresh to altered rhyolite.

6. Clast sources

The location of the Pleistocene continental ice sheets that flanked the Arctic Ocean (Prest, 1984; Grosswald, 1988, 1998; Grosswald and Hughes, 1999; Denton and Hughes, 1981; Peltier, 1994; Siegert et al., 1999; Svendsen et al., 1999) defines the possible continental source regions for glacial ice-rafted erratics in Arctic Ocean sediment. Three major circum-Arctic continental ice sheets existed. Ice sheets in north America covered northern Canada, the Laurentide ice sheet, and Greenland (Andrews, 1987; Dyke and Prest, 1989a,b; Dyke, 1999), the Eurasia ice sheet covered part of northern Russia and the Barents and Kara seas (Elverhøi et al., 1993; Polyak et al., 1995, 1997; Grosswald, 1998; Grosswald and Hughes, 1999; Siegert et al., 1999; Svendsen et al., 1999). The Late Weichselian glacial maximum reconstruction by Grosswald (1998) in the Barents and Kara Seas is considered by Svendsen et al. (1999) to be more than twice its actual size and Mangerud et al. (1999) also indicate that most of the Kara Sea was unglaciated in the Late Weichselian. However, the Taymyr Peninsula was ice covered during the early/middle Weichselian and high-resolution seismic surveys indicate that glacial sediments were deposited on the outer shelf of the western Laptev Sea during mid-Weichselian during glacial ice advances from the Taymyr Peninsula and the Severnaya Zemlya Archipelago (Kleiber et al., 1998).

Ice sheets are also reported to have covered the Laptev, East Siberian, and Chukchi Sea shelves (Denton and Hughes, 1981; Grosswald, 1988; Grosswald and Hughes 1999; Hughes and Denton, 1981; Hughes and Hughes, 1994) or the east Siberian and Laptev shelves (Peltier, 1994), but physical evidence for continental ice sheet in these areas is questionable (Svendsen et al., 1999). For example, Grosswald (1998) reports evidence of Late Weichselian glaciation in the New Siberian Islands and adjacent northern Russia and indicates that the highlands of Wrangel Island were glaciated by ice moving from the west (Grosswald and Hughes, 1999), but vibracores taken in the central and eastern Chukchi Sea to the east of Wrangel Island lack Quaternary tills or diamictites (Phillips and Colgan, 1987).

In summary the literature suggests that continental glacial ice sheets, and therefore sourcelands for the glacial erratics in the late Quaternary sediments of the Arctic Ocean were probably limited to the Eurasia ice sheet between the Taymyr Peninsula and Svalbard, and the Laurentide ice sheet between Greenland and the Mackenzie Valley of northwestern Canada on North America (Fig. 8).

6.1. Amerasia Basin

The abundance of dolostone in the late Quaternary clast suites of the Amerasia basin and the uniform and marked increase in clast abundance from the Makarov basin to the southeast Beaufort Sea indicates that the

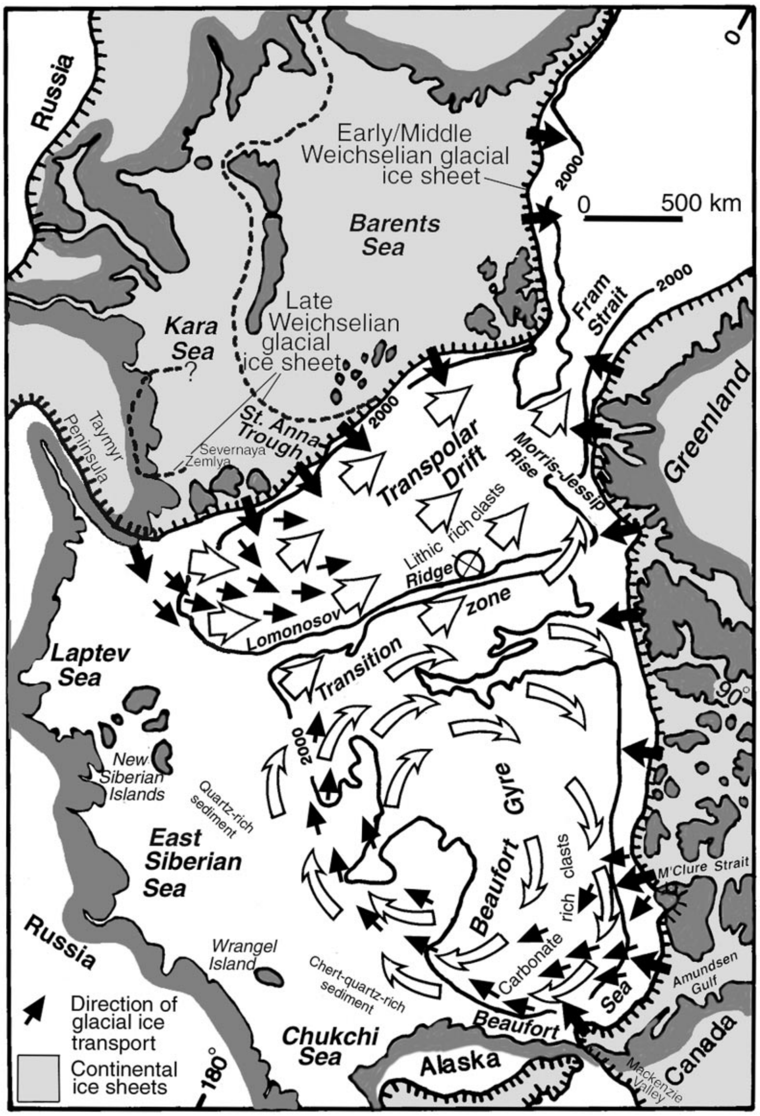

Fig. 8. Currents and glacial iceberg drift directions in the Arctic Ocean during late Pleistocene interglacial periods and boundaries of continental glacial ice sheets during Pleistocene glacial maxima. Pleistocene ice sheet boundaries for the Kara and Barents Seas during the early/middle and late Weichselian from Svendsen et al. (1999). Contours in meters.

clasts entered the Arctic Ocean in icebergs that originated in the Laurentide ice sheet of northwestern North America (Figs. 5 and 8). The regional geology of northern North America (Okulitch, 1991) along with the distribution of late Pleistocene continental ice sheets (Figs. 8 and 9) indicate that these clasts originated in the extensive dolostone-rich early Paleozoic carbonate terranes of the repeatedly glaciated northwestern Canada and the Canadian Arctic Islands. The ice streams of the Laurentide ice sheet flowed across the dolostone-rich outcrops enroute to the margin of the sea-ice sheet in the southeastern Amerasia basin and Beaufort Sea (Dyke and Prest, 1989b).

The regional geology also suggests that many of the sandstone and siltstone clasts in the southern Amerasia basin cores originated in the Sverdrup

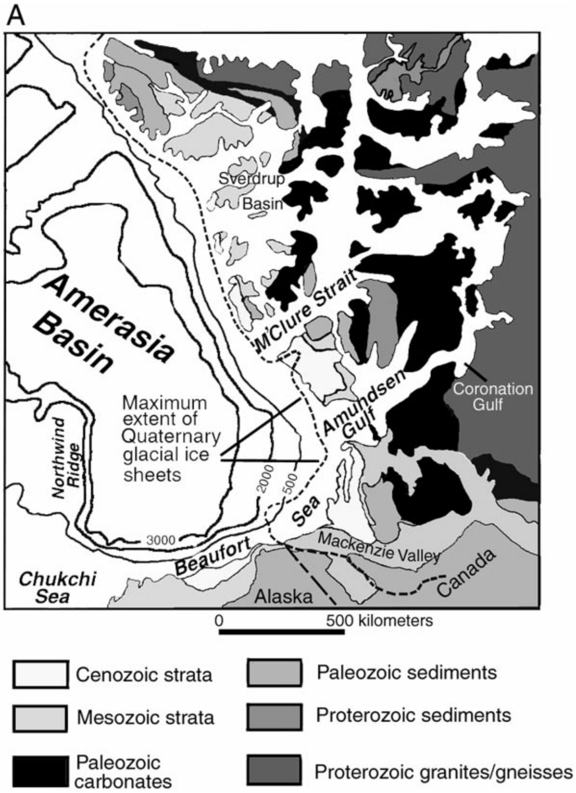

Fig. 9. Generalized geologic map of the Canadian Arctic Islands, northwestern Canada and Alaska showing that outcrops of Paleozoic dolostones and limestones in this area supplied abundant carbonate clasts to the Arctic Ocean. The maximum Pleistocene glacial ice edge from Prest (1984) and bedrock geology from Okulitch (1991).

basin and Mackenzie Valley region of northwestern Canada (Fig. 9). Distinctive red to pink granitic clasts found in cores from the Beaufort Sea and the late Pleistocene Flaxman Member of the Gubik Formation along the Beaufort Sea coast originated in the Coronation Gulf region of northwestern Canada (Rodeick, 1979), and similar clasts in cores from Northwind Ridge and the central Arctic Ocean are presumed to have the same origin. Mowatt and Naidu (1989) also indicate that gravels of the Beaufort Sea originated in the Coronation Gulf region. The source of the ice-rafted chert in the Amerasia basin sediments is in part the North American Cordillera west of the lower Mackenzie Valley (Rodeick, 1979; Bischof et al., 1996) as well as the thick Paleozoic chert-bearing formations in the Sverdrup Basin area which was overlain by the western Laurentide ice sheet.

Gravel rich in carbonate, clastic, and siliceous clasts occur repeatedly in cores from Northwind and Mendeleev Ridges in the western Arctic Ocean from the initiation of glacial ice-rafting (unit C of Clark et al., 1980) at approximately 2.7 Ma through the Holocene (Fig. 10). The similarity in clast composition and dominance of carbonate clasts in these gravels through repeated late Pliocene and Quaternary glacial-interglacial cycles supports a Canadian source for the carbonate-dominated clasts suites in our late Quaternary cores. It also implies that the current system that distributed the distinctive Amerasia clast suite across the Amerasia basin operated throughout the Quaternary.

6.2. Eurasia Basin

The specific bedrock source for the glacial ice-transported lithic-rich sediments of the eastern Arctic Ocean, the Eurasia clast suite, of Lomonosov Ridge and the Eurasia basin is uncertain. The distribution of early and middle Weichselian glaciation in the circum-Arctic indicates, however, that the sourceland lay in the northeastern part of the Eurasia ice sheet, in the Kara Sea-Taymyr Peninsula region of northern Russia (Fig. 8). The regional geology of this region (Okulitch et al., 1989) show that the abundant sandstone and siltstone clasts of the Eurasia suite could have originated in the widespread Paleozoic, Mesozoic and Tertiary sedimentary strata that underlay the Eurasia ice sheet in this region (Bogdanov et al., 1998). Spielhagen et al. (1997) suggests that the specific source of ice-rafted sediment on Lomonosov Ridge was the Taymyr Peninsula region.

Gravel rich in lithic and well rounded siliceous clasts associated with sand-rich depositional cycles are also common in piston cores from Lomonosov Ridge (Fig. 11). The similarity in lithic and siliceous clast composition in both box and piston cores on Lomonosov Ridge identifies a distinct source region that, based on core 94PC-28, had been consistently supplying lithic and siliceous clasts through multiple climate cycles. Together the persistence of the Eurasia clast suite down to the lowest beds in piston core

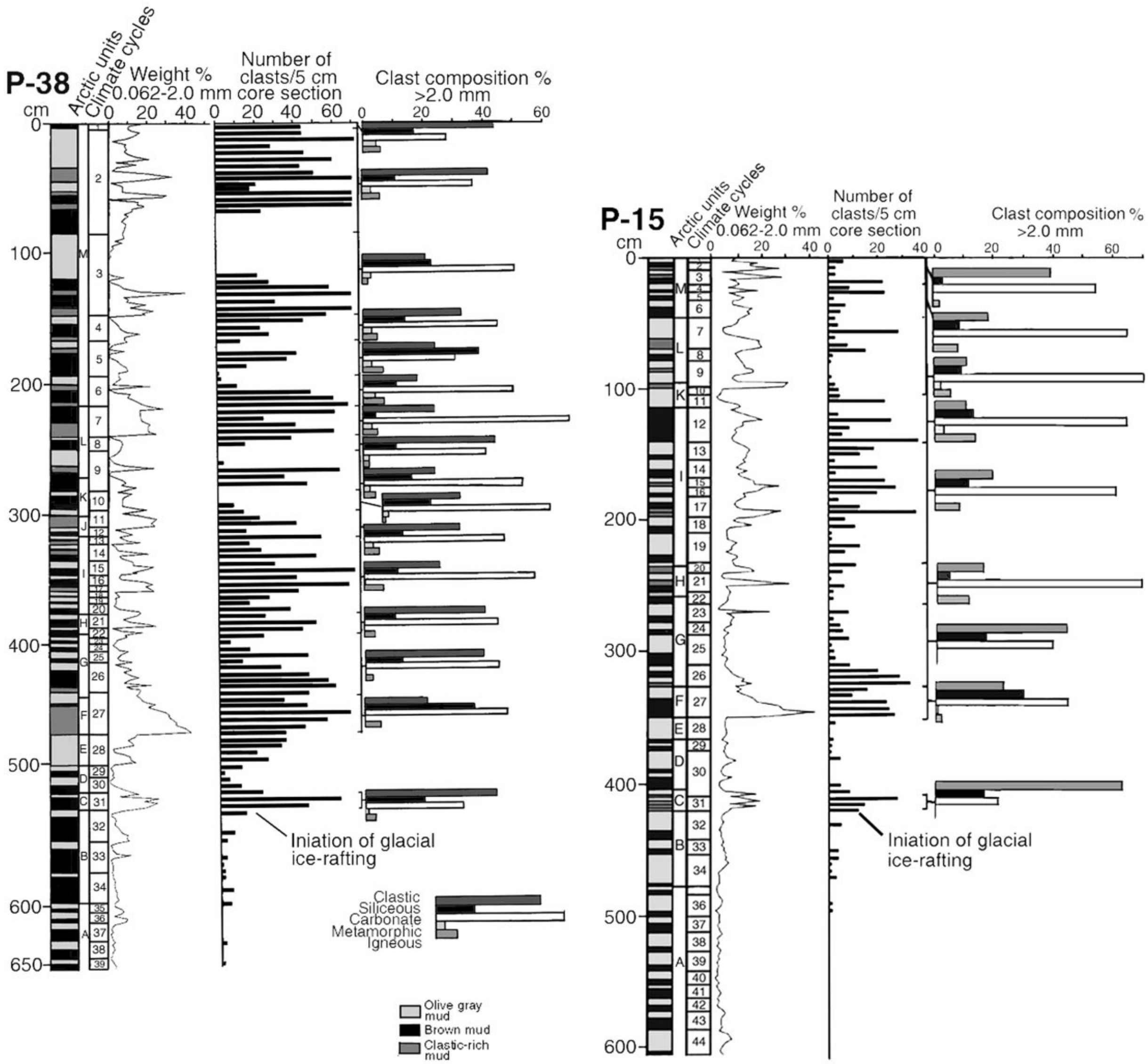

Fig. 10. Summary of climate cycles, weight percent of sand-size fraction, number of clasts >2.0 mm per 5 cm core section, and clast composition in core 92PC-38 (Northwind Ridge) and core 94PC-15 (Mendeleev Ridge) from the initiation of glacial ice-rafting in Unit C of Clark et al. (1980) to the Holocene. Arctic units are the standard lithostragraphic units of Clark et al. (1980). Clasts of the Amerasia suite were dominant throughout the history of glacial ice-rafting in the Amerasia basin, implying that westward current transport by the Beaufort Gyre operated in the Arctic Ocean during interglacial times since the initiation of glacial ice-rafting at 2.7 Ma.

94PC-28, the paucity of carbonates, and the existence of extensive sedimentary terranes in the region of the former Eurasia ice sheet that could have provided the clasts support an origin of the Eurasia clast suite in the northeastern part of Russia in the Taymyr Peninsula and Kara Sea.

The long-term persistence of the Eurasia clast suite shown by core 94PC-28 suggests that the present-day (Holocene) association of the Eurasia clast suite with the Transpolar Drift may be a long-term consequence of the surface circulation of the Eurasia basin. The Transpolar Drift may be a

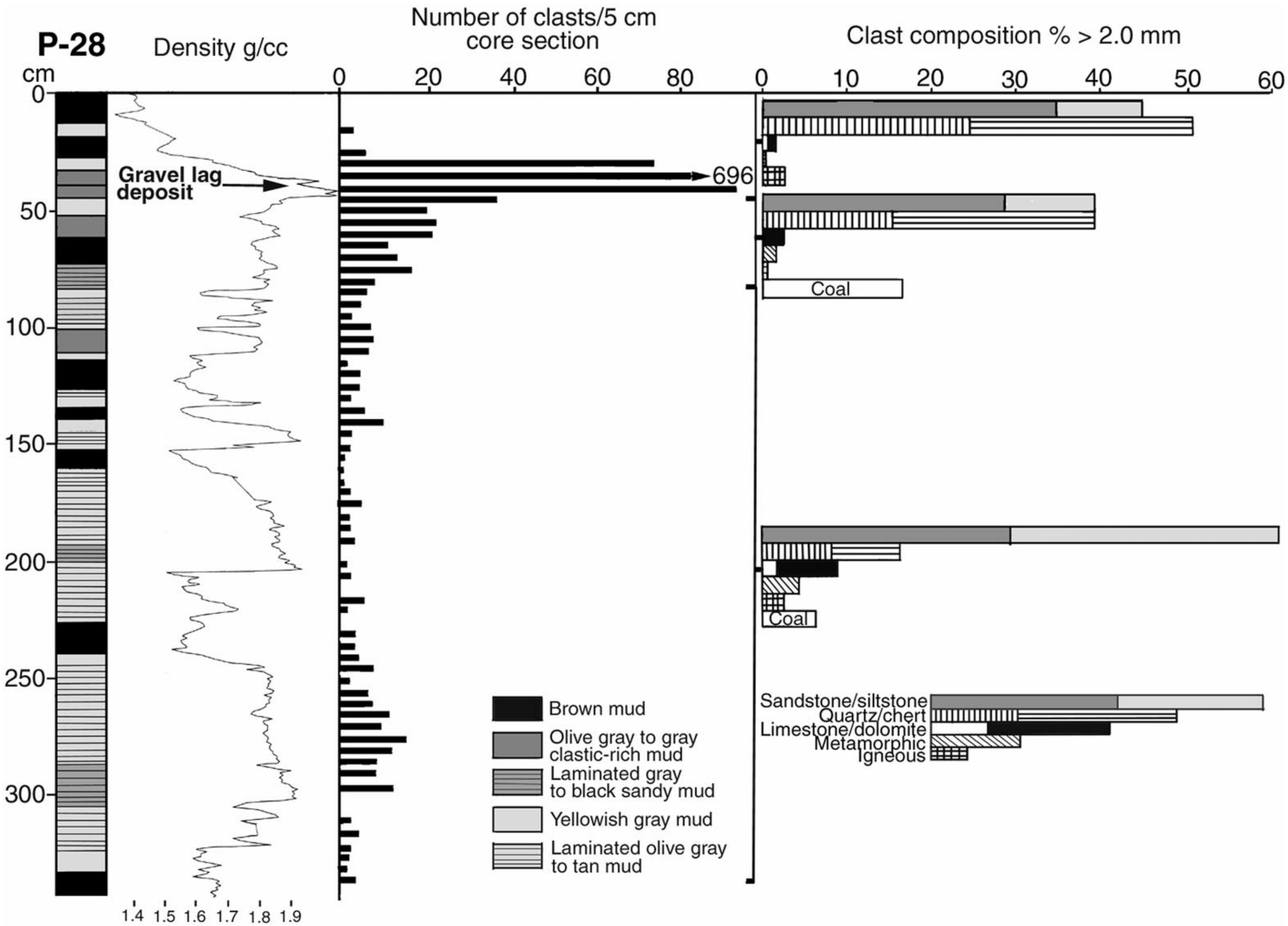

Fig. 11. Lithostratigraphy, density log, number of clasts >2.0 mm per 5 cm core sections, and clast composition of core 94PC-28, 1980 m water depth, from the Eurasia-facing flank of Lomonosov Ridge. The abundant laminations and an erosional gravel lag deposit with 696 clasts in 5 cm strata at 30 cm indicate that currents have been active at the core site and may have eroded some strata. Quartz, chert, sandstone and siltstone are the most abundant clast types within the core.

persistent feature of Arctic Ocean surface water circulation.

7. Currents and ice movement

The present mean wind driven shallow surface circulation in the Arctic Ocean, which controls the movement of sea-ice, is the clockwise Beaufort Gyre in the Amerasia basin and the Transpolar Drift in the Eurasia basin (Fig. 1). Wind-driven current reversals of up to 30 days duration of the surficial current flow and sea-ice drift are a common feature of both major current systems during late summer months in historic times (McLaren et al., 1987; Serreze et al., 1989a,b; Barry et al., 1993; Proshutinsky and Johnson, 1997). Even with current reversals in the shallow water layer, the underlying water mass moves in a clockwise direction in the Amerasia basin (Serreze et al., 1989b). Thus the 60 m thick ice island T-3, which maintained a mean clockwise movement within the Beaufort Gyre under the influence of the wind driven circulation (Jeffries, 1992), underwent numerous temporary reversals in drift direction (Browne and Cary, 1958). We expect that the glacial icebergs that entered the Arctic Ocean and the Beaufort Gyre would have behaved similarly, undergoing short lived reversals in direction but maintaining an overall mean clockwise flow.

8. Discussion

8.1. Glacial iceberg transport in the Amerasia basin

Glacial ice introduced into the Arctic Ocean by the Laurentide ice sheet entered the margins of the Arctic Ocean off northwestern Canada forming sea- and glacial-ice shelves along the margins during glacial times, when the central Arctic Ocean was covered by a thickened sheet of sea-ice. In interglacial periods, after breakup of the Arctic Ocean sea-ice sheet the glacial icebergs were free to circulate on the central Arctic Ocean progressively releasing their sediment load by melting as they moved to the west and north across the Amerasia basin. The westward and northward decrease in concentration of erratics in our sediment samples (Fig. 5) reflects a progressive reduction by melting of the total volume of erratic-bearing glacial ice introduced to the Arctic Ocean by the Laurentide ice sheet. The rate at which clast concentration decreases with distance indicates that the glacial ice decay-sedimentation function is logarithmic (Fig. 5). This is in accord with the observations of Matsumoto (1996) and Dowdeswell et al. (1995) that icebergs which contain the erratic-rich basal zones of their parent glaciers release much of their sediment load early in their decay history. Early release is fostered by the concentration of most of the erratics in such icebergs in a zone less than 10 m thick near their base, which melts first on reaching the marine environment (Dowdeswell and Murray, 1990).

Gradients in sedimentation rate and clast concentration along Northwind Ridge also indicate that glacial icebergs were concentrated along the southern margin of the Amerasia basin in late Pleistocene and Holocene time. Thus the thickness of Quaternary lithostratigraphic unit M of Clark et al. (1980) in our Northwind Ridge cores thins northward by 80%, from 340 to 65 cm, over a distance of 270 km, showing that sedimentation rates decreased northward with distance from the margin of the Canada Basin (Fig. 12). Likewise, a northward decrease of 48% in clast concentrations in cores along the crest of Northwind Ridge, from 286 to 148 clasts l^{-1} sediment over a distance of 320 km, indicates that there was also a northward decrease in the rates of deposition of glacial ice-rafted clasts in the southern Amerasia basin (Fig. 5). The northward reductions in stratigraphic unit thickness and clast concentrations indicate that the highest concentrations of glacial icebergs north of Alaska lay near the shelf break on the southern periphery of the Amerasia basin (Fig. 8). Movement of the glacial icebergs initially to the west and northwest along the margins of the Amerasia basin indicates they were carried in a current system that corresponds, in position and direction, with the modern clockwise Beaufort Gyre in that area.

The Amerasia clast suite is characterized by high proportions of carbonate, with dolostone more abundant than limestone, and proportions of sandstone and siltstone similar to, or less abundant than, carbonate. This composition indicates that the clasts were sourced in the Canadian Arctic Islands, an interpretation that is supported by a logarithmic decrease in concentration of these clasts down the trajectory of the Beaufort Grye that is uniform and continuous from high values in the eastern Amerasia basin close to the Canadian Arctic Islands to low values in the Makarov basin. The

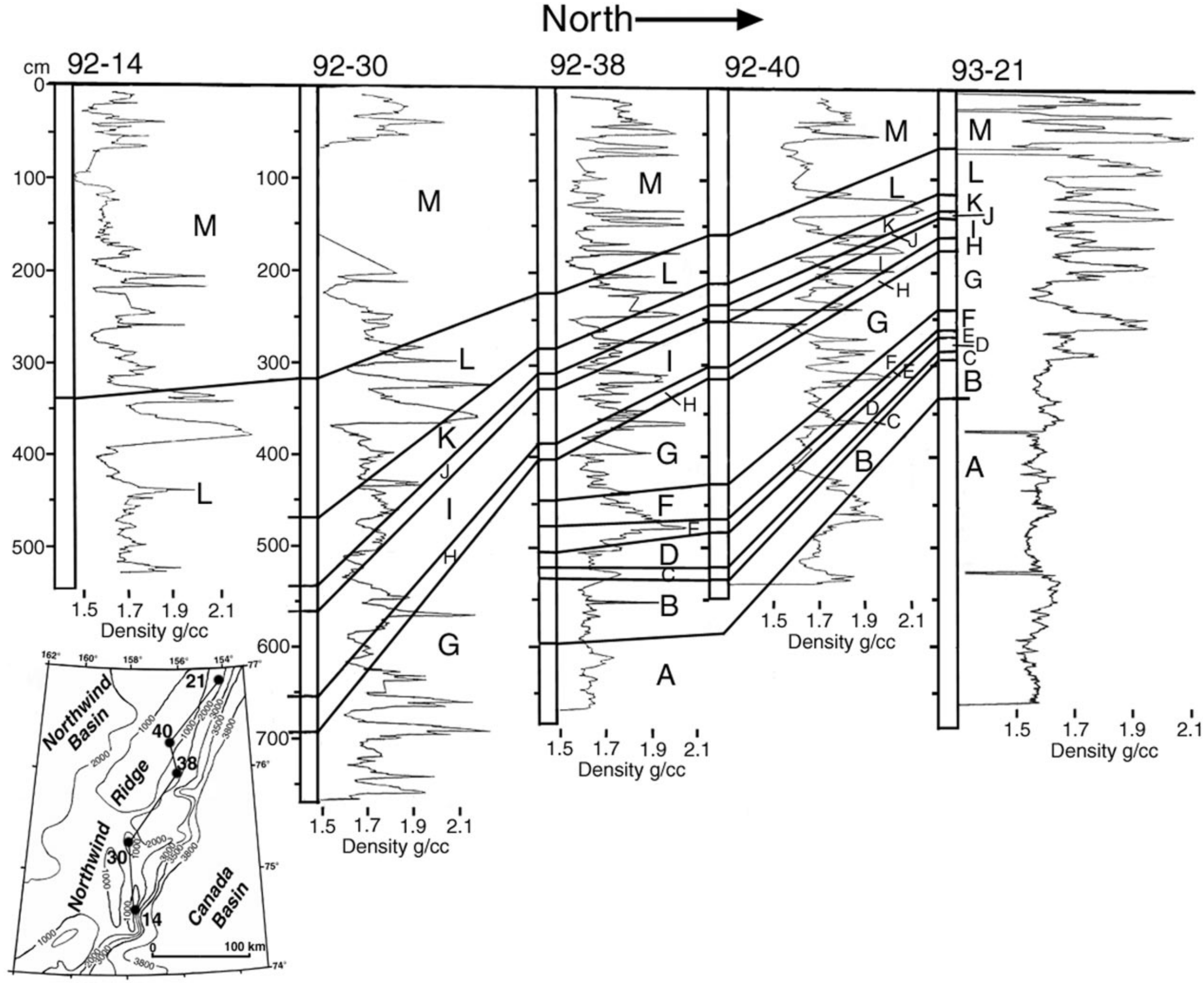

Fig. 12. Correlated Arctic lithostratigraphic units of Clark et al. (1980) and density logs of five piston cores along Northwind Ridge showing that the lithostratigraphic units thin northward. In conjunction with Fig. 5, the northward lithostratigraphic thinning indicates that IRD-bearing icebergs in the southern Amerasia basin were concentrated along the continental margins of the Beaufort and Chukchi Sea shelves in the zone of maximum rate of flow of the Beaufort Gyre (Fig. 1).

clast composition and uniform logarithmic decrease in clast concentration indicates that the Beaufort Gyre had a dominant clockwise flow back to OIS-5, the oldest sediments in our box cores. In addition, it is probable that the Beaufort Gyre, or a similar current system has operated in the Amerasia basin since the initiation of continental glaciation in the Arctic at 2.7 Ma because interglacial intervals of cores from Northwind Ridge contain only clasts of Arctic Island provenance, the Amerasia clast suite, down to the base of the Quaternary (Fig. 10).

8.2. Glacial iceberg transport in the Eurasia basin

Glacial ice was also introduced into the Transpolar Drift and the Arctic Ocean from a late Weichselian ice sheet that covered the Barents shelf and Novaya Zemlya of northern Russia. These icebergs derived from the late Weichselian glaciers moved toward Fram strait (Vogt et al., 1994) and apparently not northward toward Lomonosov Ridge. However, the early/middle Weilchselian ice sheet was more extensive and covered the Barents and Kara shelves as well

as the Taymyr Peninsula (Fig. 8). Glacial ice streams originating in this ice sheet were discharged through St. Anna Trough and may at times reached Lomonosov Ridge. Glaciers from the Taymyr Peninsula region formed marine ice sheets on the adjacent shelf regions (Spielhagen et al., 1997) and supplied icebergs which moved northwest to Lomonosov Ridge. Evidence for glaciation derived possibly from the Taymyr Peninsula-Laptev Sea region and/ or adjacent ice shelves is supported by iceberg grounding to depths of 1000 m on Lomonosov Ridge crest between 85°20′ and 86°10′ (Polyak et al., 1999; Jakobsson, 2000). Base on the directional trends of the ice gouges the deep draft ice that produced the gouges may have originated from either the area between Svalbard and Franz Josef's Land or the Arlis Plateau (Jakobsson, 2000).

8.3. Transition zone

The uniform and continuous decrease in both the concentration and composition of the >2 mm clast fraction in the Amerasia basin cores from the Arctic Islands to the central Arctic is abruptly terminated at the south flank of Lomonosov Ridge, where the abundance of clasts increases abruptly from 10–31 clasts l^{-1} of sediment. This abrupt increase in clast concentration is accompanied by a change in the bulk composition of the carbonate-rich Amerasia clast suite in which dolostone is more common than limestone, to the Eurasia clast suite, in which sandstone and siltstone greatly predominant over carbonate and limestone is usually more abundant than dolostone.

The concomitant changes in clast concentration and composition occur near the modern boundary between the Beaufort Gyre and the Transpolar Drift, indicating that these major current systems of the Arctic Ocean and their boundary zone have remained in approximately their present positions during successive interglacial intervals in the Arctic Ocean since at least the late Pleistocene. The boundary between the two current systems may have fluctuated laterally through time, however, as indicated by the presence of detrital carbonate clasts on Lomonosov Ridge and in the Eurasia basin (Spielhagen et al., 1997; Nørgaard-Pedersen, 1997). We acknowledge that Paleozoic carbonate bedrock is also reported from Novaya Zelyma and the Taymyr Peninsula (Nørgaard-Pedersen, 1997) and may have contributed clasts by glacial icebergs to the Eurasia basin, but, their limited outcrop area compared to the extensive carbonate terranes of northwest Canada and the Canadian Arctic Islands suggests that the contribution was minimal. Spielhagen et al. (1997) indicates that at times glacial ice in the Eurasia basin may have restricted or prevented icebergs from the Beaufort Gyre from entering the Eurasia basin. However, detrital carbonate values in Lomonosov Ridge cores of up to 60% back to 2.7 Ma (Spielhagen et al., 1997) suggests to us that at times substantial detrital carbonate was transported into the Eurasia basin by the Beaufort Gyre.

Our box and piston cores suggest that the Beaufort Gyre and Transpolar Drift were active at least during interglacial times, back to the late Quaternary, and perhaps to 2.7 Ma. Because the clockwise Beaufort Gyre is presumed to be driven by the anticyclonic Arctic high pressure system that overlies the Beaufort Sea north of Alaska (Kolatschek et al., 1996), our data also suggests that the Arctic high in something like its present configuration has a similar antiquity. This hypothesis is supported by the morphology of eolian dunes in an extensive sand sea that overlies 11,600 km^2 of the Arctic Coastal Plain of the North Slope of Alaska. The symmetry and age of these dunes (Carter, 1981, 1983; Dinter et al., 1990; Galloway and Carter, 1993) indicate that the dominant wind direction in coastal Arctic Alaska during the late Wisconsin last glacial maximum (LGM) and Holocene was east–northeast to west–southwest, with occasional 180° reversals.

In addition, thaw lakes of Holocene age on the Arctic Coastal Plain are oriented with their long axes trending N 10° to 15° W, normal to the dominant east–northeast to west–southwest and secondary west–southwest to east–northeast wind directions on the Coastal Plain. Carson and Hussey (1962) have shown that the prevailing winds have developed sublittoral shelves and sand bars on the east and west sides of these lakes that protect them from thaw and erosion, whereas, the unprotected north and south ends continue to erode, thereby elongating the lakes normal to the dominant east–northeast to west–southwest wind direction.

The evidence for westward migrating eolian dunes

during the LGM and thaw lake orientation show that the late Wisconsin and Holocene wind direction on the Arctic Coastal Plain was dominantly from the east–northeast. The westerly-directed air flow, in conjunction with the evidence for the clockwise circulation of glacial icebergs in the Amerasia basin during late Quaternary interglacials suggest that an anticyclonic high pressure system existed north of Alaska since the late Wisconsin. This conflicts with the conclusion of Bischof and Darby (1997) that the wind-driven circulation in the Arctic in the past was different from that of today and that the ice drift pattern was not compatible with the clockwise flowing Beaufort Gyre. However, the westerly eolian dune migration across northern Alaska, in conjunction with the current directions in the Amerasia basin indicated by variations in clast size and composition in Arctic sediment cores indicates that an anticlonic high persisted over the Amerasia basin driving the Beaufort Gyre and that this high was the dominant driver of ice movement in the region since as least the LGM, and probably since OIS-5 and earlier.

9. Conclusions

1. The Beaufort Gyre and the Transpolar Drift current systems have apparently existed in the Arctic Ocean since at least the late Pleistocene (OIS-5), the age of the oldest beds in our box cores.
2. The highest concentration of glacial ice-rafted clasts >2.00 mm are found in the southeastern Canada basin adjacent to the Laurentide ice sheet decreasing by 98% in the Makarov basin near Lomonosov Ridge.
3. Glacial ice-rafted sediment in the Arctic Ocean contains two distinct clast assemblages, an Amerasia suite containing of up to 70% detrital carbonate, and up to 46% micaceous sandstone/siltstone and an Eurasia suite composed of up to 78% sandstone/siltstone, along with up to 52% siliceous clasts. An abrupt transition between these suites occurs in the vicinity of the Amerasia flank of Lomonosov Ridge.
4. The abrupt decrease in detrital carbonate clasts and abrupt increase in sandstone and siliceous clasts at the Amerasia flank of Lomonosov Ridge is consistent with a sharp increase in clast concentrations in the box cores. These changes mark the transition zone between the major surface current systems of the Arctic Ocean, the Beaufort Gyre of the Amerasia basin and the Transpolar Drift of the Eurasia basin.
5. The boundary between the Beaufort Gyre and the Transpolar Drift fluctuated, resulting in an apparent transition zone over the northern Makarov basin and Lomonosov Ridge in which mixing of the carbonate-rich (Amerasia suite) and sandstone-rich (Eurasia suite) clast suites occurred.
6. Clasts of the Amerasia basin suite in our cores exhibit a logarithmic decrease in abundance to the west and northwest, which resembles a glacial iceberg melting function and supports distribution by glacial icebergs in the Beaufort Gyre. A corresponding northward decrease in both clast abundance and lithostratigraphic unit thickness on Northwind Ridge, across the clockwise flow of the gyre, shows that the glacial icebergs in the Beaufort Gyre were concentrated along the southern margin of the Amerasia basin.
7. Comparison of the Amerasia and Eurasia clast suite with the character of bedrock and the distribution of the Pleistocene continental glacial ice sheets in the circum Arctic land masses indicates that the Amerasia basin clast suite originated in the Canadian Arctic Islands and that the Eurasia basin clast suite probably originated in the Taymyr Peninsula and Kara-Barents Sea region.
8. The carbonate-rich Amerasia basin suite existed back to the initiation of glacial ice-rafting in the Arctic Ocean implying that the Beaufort Gyre has existed since 2.7 Ma (mid-late Pliocene).

Acknowledgements

This study is based on cores collected from the US Coast Guard Cutters *Polar Sea* in a polar transect from July to September, 1994 and from the US Coast Guard Cutter *Polar Star* in the Canada basin in 1988, 1989, 1992, and 1993. We are grateful to the Coast Guard for the opportunity to work from the *Polar Star*, and *Polar Sea* and to Captains L. Bringham, P.R. Taylor, R. Hammon, P. Hagstrom, and R.J.

Parsons and the ship's complements for the assistance and many courtesies extended to us during field operations, which in most years were conducted under severe sea-ice conditions. We also thank Lisa M. Clough, East Carolina University for sharing her sampling equipment. David L. Clark examined our 1992 piston cores and established the litho-stratigraphy for core 38, for which we are grateful. Comments by Peter Barnes, Walter Barnhardt, Lenoid Polyak, Niels Nørgaard-Pederson, Tore Vorren, and two anonymous reviewers significantly improved the manuscript. The work was funded by the US Geological Survey's Global Change and Climate History Program.

References

Andrews, J.T., 1987. The late Wisconsin glaciation and deglaciation of the Laurentide Ice Sheet. In: Ruddiman, W.F., Wright, Jr., H.E. (Eds.), North America and adjacent oceans during the last deglaciation. The Geology of North America. The Geological Society of America, Boulder, CO., K-3 13-37.

Barry, R.G., Serreze, M.C., Maslanik, J.A., Prellerl, R.H., 1993. The Arctic sea ice-climate system: observations and modeling. Reviews of Geophysics 31, 397–422.

Bischof, J., 1990. Dropstones in the Norwegian–Greenland Sea - Indications of Late Quaternary circulation Patterns? In: Beil, U., Thiede, J. (Eds.), The Geological history of Cenozoic Polar Oceans: Arctic verses Antarctic, NATO ASI Ser. C, 308, 499–518.

Bischof, J., Clark, D.L., Vincent, J.-S., 1996. Origin of ice-rafted debris: Pleistocene paleoceanography in the western Arctic Ocean. Paleoceanography 11, 743–756.

Bischof, J.F., Darby, D.A., 1997. Mid- to late Pleistocene ice drift in the western Arctic Ocean: evidence for a different circulation in the past. Science 277, 74–78.

Bogdanov, N.A., Khain, V.E., Rosen, O.M., Shipilov, E.V., Vernikovsky, V.A., Drachev, S.S., Kostyuchenko, S.L., Kuz'michev, A.B., Sekretov, S.B., 1998. Tectonic Map of the Kara and Laptev Seas and northern Siberia. Scale 1:2,500,000. Institute of the Lithosphere of Marginal Seas, Russian Academy of Sciences, Moscow, 127.

Browne, I.M., Cary, A.P., 1958. The movement of ice in the Arctic Ocean. Arctic Sea Ice, National Academy of Science, Washington, D. C. 598, 191–209.

Clark, D.L., 1971. Arctic Ocean ice cover and its late Cenozoic history. Geological Society of America Bull. 82, 3313–3324.

Clark, D.L., Hanson, A., 1983. Central Arctic Ocean sediment texture: a key to ice transport mechanisms. In: Molnia, B.F. (Ed.). Glacial-marine Sedimentation. Plenum, New York, pp. 301–330.

Clark, D.L., Whitman, R.R., Morgan, K.A., Mackay, S.D., 1980. Stratigraphy and glacial-marine sediments of the Amerasian Basin, central Arctic Ocean. Geological Society of America, Special Paper 181, 1–57.

Carson, C.E., Hussey, K.M., 1962. The oriented lakes of Arctic Alaska. J. of Geology 70, 417–439.

Carter, L.D., 1981. A Pleistocene sand sea on the Alaskan Arctic Coastal Plain. Science 221, 381–383.

Carter, L.D., 1983. Fossil sand wedges on the Alaskan Arctic Coastal Plain and their paleoenvironmental significance. In: Permafrost, Fourth International Conference Proceedings: Washington DC, National Academy Press, 9–114.

Clark, D.L., 1990. Arctic Ocean ice cover; geologic history and climatic significance. In: Grantz, A., Johnson, L., Sweeney, J.F. (Eds.), The Arctic Ocean Region. The Geology of North America, Vol. L. Geological Society of America, Boulder, CO, pp. 53–62.

Colony, R., Thorndike, A.S., 1984. An estimate of the mean field of Arctic sea ice motion. J. of Geophysical Research 89, 10623–10639.

Darby, D.A., Bischof, J., 1996. A statistical approach to source determination of lithic and Fe oxide grains: an example from the Alpha Ridge, Arctic Ocean. J. of Sedimentary Research 66, 599–607.

Darby, D.A., Bischof, J., Jones, G.A., 1997. Radiocarbon chronology of depositional regimes in the western Arctic Ocean. Deep-Sea Research 44, 1745–1757.

Denton, G.H., Hughes, T.J., 1981. The Arctic ice sheet: an outrageous hypothesis. In: Denton, G.H., Hughes, T.J. (Eds.). The Last Great Ice Sheets. Wiley and Sons, New York, pp. 437–467.

Dinter, D.A., Carter, L.D., Brigham-Grette, J., 1990. Late Cenozoic geologic evolution of the Alaskan North Slope and adjacent continental shelves. In: Grantz, A., Johnson, G.L., Sweeney, J.F. (Eds.), The Arctic Ocean region. The Geology of North America. Boulder, Colorado, Geological Society of America, L, 459–490.

Dowdeswell, J.A., Maslin, M.A., Andrews, J.T., McCave, I.N., 1995. Iceberg production, debris rafting, and the extent and thickness of Heinrich layers (H-1, H-2) in North Atlantic sediments. Geology 23, 301–304.

Dowdeswell, J.A., Murray, T., 1990. Modeling rates of sedimentation from icebergs. In: Dowdeswell, J.A., Scourse, J.D. (Eds.), Glaciomarine environments: processes and sediments. Geological Society of London special publication 53, 121–137.

Dyke, A.S., 1999. Last glacial maximum and deglaciation of Devon Island, Arctic Canada: support for an Innuitian ice sheet. Quaternary Science Reviews 18, 393–420.

Dyke, A.S., Prest, V.K., 1989a. Retreat of the Laurentide ice sheet during the upper Wisconsin and Holocene. Geol. Survey of Canada Chart 1702A.

Dyke, A.S., Prest, V.K., 1989b. Paleogeography of northern North America between 18,000 and 5,000 years before the present. In: Fulton, R.J. (Ed.), The Quaternary of Canada and Greenland. The Geology of North America. The Geological Society of America, Boulder, Colorado, K-1, 1:12,500,000, 3 sheets.

Eisenhauer, A., Spielhagen, R.F., Frank, M., Hentzschel, G., Mangini, A., Kubik, P.W., Dittrich-Hannen, B., Billen, T., 1994. ^{10}Be records of sediment cores from high northern

latitudes: implications for environmental and climate changes. Earth and Planetary Science Letters 124, 171–184.

Elverhøi, A., Fjeldskaar, W., Solheim, A., Nyland-Berg, M., Russwurm, L., 1993. The Barents Sea ice sheet-A model of its growth and decay during the last ice maximum. Quaternary Science Reviews 12, 863–873.

Galloway, J.P., Carter, L.D., 1993. Paleowind direction for late Holocene dunes on the western Arctic Coastal Plain, Northern Alaska. In: Till, A.B., Moore, T.E. (Eds.), Geologic studies in Alaska by the US Geological Survey, 1993. US Geological Survey Bulletin 2107, 27-30.

Gard, G., 1988. Late Quaternary calcareous nannofossils biozonation, chronology and paleo-oceanography in areas north of the Faeroe-Iceland Ridge. Quaternary Science Reviews 2, 63–73.

Grosswald, M.G., 1988. Antarctic-style ice sheet in the Northern Hemisphere: toward the new global glacial theory. Polar Geography and Geology 12, 239–267.

Grosswald, M.G., 1998. Late-Weichselian ice sheets in Arctic and Pacific Siberia. Quaternary International 45/46, 3–18.

Grosswald, M.G., Hughes, T.J., 1999. The case for an ice shelf in the Pleistocene Arctic Ocean. Polar Geography 23, 23–54.

Hughes, T., Denton, G.H., 1981. The Arctic ice sheet: an outrageous hypothesis. In: Denton, G.H., Hughes, T.J. (Eds.). The Last Great Ice Sheets. Wiley and Sons, New York, pp. 440–467.

Hughes, B.A., Hughes, T.J., 1994. Transgressions: rethinking Beringian glaciation. Palaeogeography, Palaeoclimatology, Palaeoecology 110, 275–294.

Ishman, S.E., Polyak, L.V., Poore, R.Z., 1996. Expanded record of Quaternary oceanographic change: Amerasian Arctic Ocean. Geology 24, 139–142.

Jakobsson, M., Løvlie, R., Al-Hanbali, H., Aarnold, E., Backman, J., Morth, M., 2000. Manganese and color cycles in Arctic Ocean sediments constrain Pleistocene chronology. Geology 28, 23–26.

Jakobsson, M., 2000. Mapping the Arctic Ocean: bathymetry and Pleistocene paleoceanography. Department of Geology and Geochemistry, Stockholm University, No. 306 93.

Jeffries, M.O., 1992. Arctic ice shelves and ice islands: origin growth and disintegration, physical characteristics, structural-stratigraphic variability, and dynamics. Reviews of Geophysics 30, 245–267.

Kolatschek, J., Eicken, H., Alexandrov, V. Yu., Kreyscher, M., 1996. The sea-ice cover of the Arctic Ocean and the Eurasian marginal seas: a brief overview of present day patterns and variability. In: Stein, R., Ivanov, G.I., Levitan, M.A., Fahl, K. (Eds.), Reports on Polar research: surface–sediment composition and sedimentary processes in the central Arctic Ocean and along the Eurasian continental margin. Alfred-Wegener-Institute for Polar and marine research 212, 2–18.

Kleiber, H.P., Niessen, F., Weiel, D., 1998. The Late Quaternary evolution of the western Laptev Sea continental margin – implications from sub-bottom profiling. American Geophysical Union, EOS, Transactions 79, 501.

Landa, E.W., Reimnitz, E., Beals, D.M., Pochkowsski, J.M., Winn, W.G., Rigor, I., 1998. Transport of ^{137} and ^{239,240}Pu with ice-rated debris in the Arctic Ocean. Arctic 51, 27–39.

Mangerud, J., Svendsen, J.I., Astakhov, V.I., 1999. Age and extent of the Barents and Kara ice sheets in northern Russia. Boreas 28, 46–80.

Matsumoto, K., 1996. An iceberg drift and decay model to compute the ice-rafted debris and iceberg meltwater flux: application to the interglacial North Atlantic. Paleoceanography 11, 727–742.

McLaren, A.S., Serreze, M.C., Barry, R.G., 1987. Seasonal variations of sea ice motion in the Canada Basin and their implications. Geophysics Research Letters 14, 1123–1126.

Mowatt, T.C., Naidu, A.S., 1989. Nature and source of gravel in sediments from Alaska continental shelf. Beaufort Sea, Arctic Ocean. 28th International Geological Congress, Washington, DC, 271–272.

Nørgaard-Pedersen, N., 1997. Late Quaternary Arctic Ocean sediment records: surface ocean conditions and provenance of ice-rafted debris. GEOMAR report 65, 1–115.

Nørgaard-Pedersen, N., Spielhagen, R.F., Thied, J., Kassens, H., 1998. Central Arctic surface ocean environment during the past 80,000 years. Paleoceanography 13, 193–204.

Nürnberg, D., Wollenburg, I., Dethliff, D., Eicken, H., Kassens, H., Letzig, T., Reimnitz, E., Thiede, J., 1994. Sediments in Arctic sea ice: implications for entrainment, transport and release. Marine Geology 119, 185–214.

Okulitch, A.V., Lopatin, B.G., Jackson, H.R., 1989. Circumpolar geological map of the Arctic. Geological Survey of Canada, Map 1765 A, Scale 1:6,000,000.

Okulitch, A.V. (compiler) 1991. Geology of the Canadian Archipelago and North Greenland. In: Trettiln, H.P. (Ed.), Innuitian orogen and Arctic Platform: Canada and Greenland. The Geology of North America. The Geological Society of America, Boulder, Colorado, E, 1:200,000.

Peltier, W.R., 1994. Ice age paleotopography. Science 265, 195–201.

Pfirman, S., Gascard, J.C., Wollenburg, I., Mudie, P., Abelmann, A., 1989. Particle-laden Eurasian Arctic sea ice: observations from July and August 1987. Polar Research 7, 59–66.

Pfirman, S., Lange, M.A. Wollenburg, I., Schlosser, P., 1990. Sea ice characteristics and the role of sediment inclusions in deep-sea deposition: Arctic–Antarctic comparison. In: Beil, U., Thiede, J. (Eds.), Geological history of the Polar Oceans: Arctic versus Antarctic, NATO ASI Ser., C 308, 187–211.

Phillips, R.L., Colgan, M.W., 1987. Vibracore stratigraphy of the northeastern Chukchi Sea. In: Hamilton, T.D., Galloway, J.P. (Eds.), Geologic studies in Alaska, 1986, US Geological Survey Circular 998, 157–160.

Phillips, R.L., Grantz, A., Mullen, M.W., Rieck, H.J., McLaughin, M.W., Selkirk, T.L., 1992. Summary of lithostratigraphy and stratigraphic correlations in piston cores from Northwind Ridge. Arctic Ocean, from USCGC Polar Star, 1988. US Geological survey Open-file Report. 92-426 1–110.

Phillips, R.L., Grantz, A., 1997. Quaternary history of sea ice and paleoclimate in the Amerasia basin, Arctic Ocean, as recorded in the cyclical strata of Northwind Ridge. Geological Society of America Bulletin 109, 2–16.

Polyak, L., Lehman, S.J., Gataullin, V., Jull, A.J.T., 1995. Two-step deglaciation of the southeastern Barents Sea. Geology 23, 567–571.

Polyak, L., Forman, S.L., Herlihy, F.A., Ivanoc, G., Krinitsky, P., 1997. Late Weichselian deglacial history of the Svyataya (Saint) Anna Trough, northern Kara Sea, Arctic Russia. Marine Geology 143, 169–188.

Polyak, L., Edwards, M.H., Jakobsson, M., Coakley, B.J., 1999. Glacial scouring in the deep Arctic Ocean: evidence from the Chukchi Plateau and the Lomonosov Ridge. American Geophysical Union, EOS, Transactions 80, 1000–1001.

Poore, R.Z., Phillips, R.L., Rieck, H.J., 1993. Paleoclimate record for Northwind Ridge, western Arctic Ocean. Paleoceanography 8, 149–159.

Poore, R.Z., Osteerman, L., Curry, W.B., Phillips, R.L., 1999. Late Pleistocene and Holocene meltwater events in the western Arctic Ocean. Geology 27, 759–762.

Prest, V.K., 1984. Late Wisconsin glacier complex. Map 1257A, Geol. Surv. of Can., Ottawa, Ont.

Proshutinsky, A.Y., Johnson, M.A., 1997. Two circulation regimes of the wind-driven Arctic Ocean. Journal Geophysical Research 102, 12493–12514.

Rigor, I., 1992. Arctic Ocean buoy program. ARGOS Newsletter 44, 1–3.

Rodeick, C.A., 1979. The origin, distribution, and depositional history of gravel deposits on the Beaufort Sea continental shelf, Alaska. US Geological Survey Open-File Report. 79-234 1-83.

Reimnitz, E., Marincovich Jr., L., McCormic, M., Briggs, W.M., 1992. Suspension freezing of bottom sediment and biota in the Northwest Passage and implications for Arctic Ocean sedimentation. Canadian Journal Earth Science 29, 693–703.

Schwarzacher, W., Hunkins, H., 1961. Dredged gravels from the central Arctic Ocean. In: Raasch, G.O. (Ed), Geology of the Arctic: Proceedings of the 1st International Symposium on Arctic Geology 1, 668–677.

Serreze, M.C., McLaren, A.S., Barry, R.G., 1989a. Seasonal variations of sea ice motion in the Transpolar Drift Stream. Geophysics Research Letters 16 (8), 811–814.

Serreze, M.C., Barry, R.G., McLaren, A.S., 1989b. Seasonal variations of sea ice motion and effects on sea ice concentration in the Canada basin. J. of Geophysical Research 94 (C8), 10955–10970.

Siegert, M.J., Dowdeswell, J.A., Melles, M., 1999. Late Weichselian glaciation of the Russian high Arctic. Quaternary Research 52, 273–285.

Spielhagen, R.F., Eisenhyauer, A., Frank, M., Frederichs, T., Kassens, H., Mangini, A., Nowaczyk, N.R., Nørgaard-Pedersen, N., Schaper, S., Stein, R., Thiede, J., Tiedemann, R., Wahsner, M., Bonani, G., Kubik, P.W., 1997. Arctic Ocean evidence for Late Quaternary initiation of northern Eurasia ice sheets. Geology 25, 783–786.

Stein, R., 1996. Organic-carbon and carbonate distribution in Eurasian continental margin and Arctic Ocean deep-sea surface sediments: sources and pathways. In: Stein, R., Ivanov, G.I., Levitan, M.A., Fahl, K. (Eds.), Reports on Polar research: surface–sediment composition and sedimentary processes in the central Arctic Ocean and along the Eurasian continental margin. Alfred-Wegener-Institute for Polar and marine research 212, 243–267.

Svendsen, J.I., Astakhov, V.L., Bolshiyanov, B.T., Demidov, I., Dowdeswell, J.A., Gataullin, V., Jhort, C., Hubberten, H.W., Larsen, E., Mangerud, J., Mellesl, M., Moller, P., Saarnisto, M., Siegert, M.J., 1999. Maximum extent of the Eurasian ice sheets in the Barents and Kara Sea region during the Weichselian. Boreas 28, 234–242.

Vassmyr, S., Vorren, T.O., 1990. Clast petrography and stratigraphy in Late Quaternary sediments in the southwestern Barents Sea. Norsk Geologisk Tidsskrift 70, 95–110.

Vogt, C., 1996. Bulk mineralogy in surface sediments from the eastern central Arctic Ocean. In: Stein, R., Ivanov, G.I., Levitan, M.A., Fahl, K. (Eds.), Reports on Polar research: surface–sediment composition and sedimentary processes in the central Arctic Ocean and along the Eurasian continental margin. Alfred-Wegener-Institute for Polar and marine research 212, 159–171.

Vogt, P.R., Crane, K., Sundvor, E., 1994. Deep Pleistocene iceberg plowmarks on the Yermak Plateau: sidescan and 3.5 kHz evidence for thick calving ice fronts and a possible marine ice sheet in the Arctic Ocean. Geology 22, 403–406.